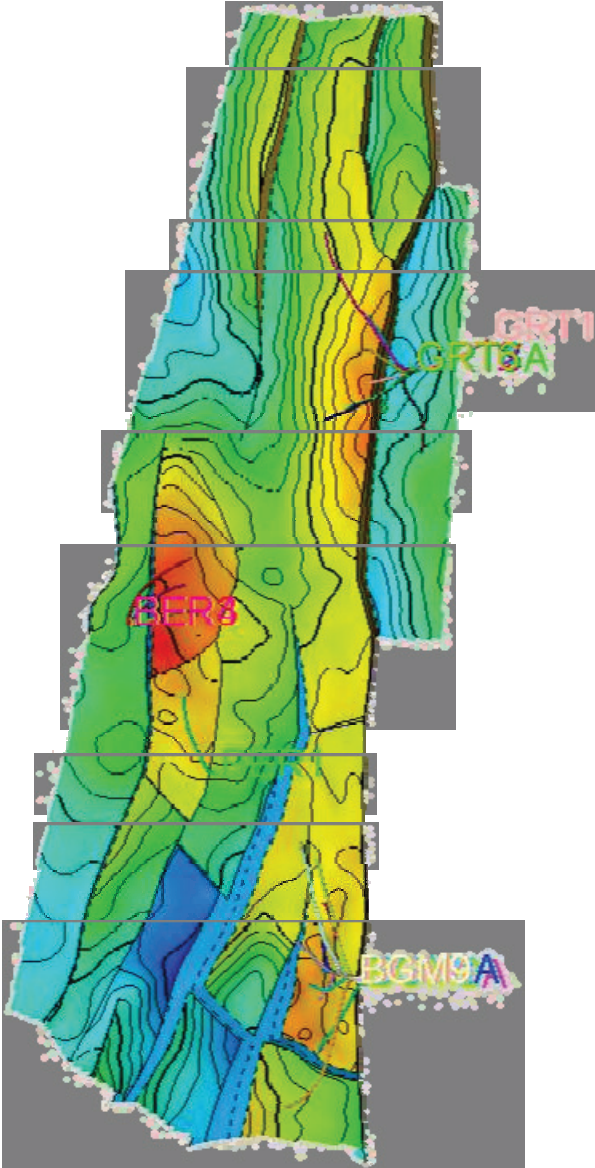


BERGERMEER UGS MODELLING STUDY, PHASE 2



Taqa Energy BV

BERGERMEER UGS MODELLING STUDY, PHASE 2

March 2008

PREPARED

Taqa Energy BV

Bezuidenhoutseweg 74
The Hague
The Netherlands

BY

Horizon Energy Partners BV

Prinses Margrietplantsoen 81
2595 BR The Hague
The Netherlands

NAME

SIGNED

DATE

PREPARED BY

Jeroen Mullink

Hans Martens

APPROVED BY

Table of Contents

LIST OF TABLES	6
LIST OF FIGURES	8
EXECUTIVE SUMMARY	17
1 INTRODUCTION	18
2 UGS INPUTS	21
2.1 PHASE 1 FINDINGS & MODEL DESCRIPTION	21
2.2 UGS STORAGE SPECIFICATIONS	25
2.3 SUBSURFACE MODEL & REALIZATIONS	25
2.4 WELL TEST DATA	29
2.5 HISTORY MATCHING ALTERNATES	33
3 WELL PERFORMANCE MODELLING	40
3.1 INFLOW PERFORMANCE MODEL BGM-1	40
3.2 VLP / IPR MATCHING BGM-1	41
3.3 DESCRIPTION OF NON-DARCY SKIN IN ECLIPSE	42
3.4 LIFT CURVES.....	44
3.5 FRICTION VERSUS GRAVITY LOSSES IN TUBING (PRESSURE VS DEPTH)	47
3.6 IPR / VLP SENSITIVITIES	48
3.6.1 <i>Skin</i>	48
3.6.2 <i>Permeability</i>	49
3.6.3 <i>CGR</i>	51
3.6.4 <i>WGR</i>	52
3.6.5 <i>Tubing roughness</i>	54
3.6.6 <i>Tubing diameter</i>	55
3.6.7 <i>Summary</i>	57
4 SUMMER INJECTION TEST INTERPRETATION	59
4.1 SUMMER INJECTION TEST FORECASTS.....	59
4.2 INJECTION TEST DATA OVERVIEW	60
4.3 SUMMER INJECTION TEST INTERPRETATION	64
4.4 CALIBRATION OF DYNAMIC MODEL TO SUMMER INJECTION TEST RESULTS	68
4.5 GWC MOVEMENTS SUMMER INJECTION TEST.....	73
5 UGS FORECASTING	76
5.1 DEVELOPMENT SCENARIOS.....	76

5.2	SUBSURFACE REALISATIONS.....	76
5.3	WELL PLANNING.....	77
5.4	FORECAST RESULTS MODEL DISMIDHIGHKV	81
5.4.1	<i>Tubing size</i>	83
5.4.2	<i>GWC</i>	84
5.5	FORECAST RESULTS BELL_050 AND BELL_033 MODELS	88
5.6	FIELD PERFORMANCE CURVES	91
5.7	FORECAST SENSITIVITIES	97
5.7.1	<i>Influence of heterogeneity and well positioning</i>	97
5.7.2	<i>Forecast sensitivities summary</i>	104
5.7.3	<i>Groet</i>	106
5.7.4	<i>Local Grid Refinement</i>	108
5.8	DRILLING AND FILLING UP SEQUENCE	111
5.9	END-OF-FIELD-LIFE	112
6	SUMMARY AND RECOMMENDATIONS	114
	REFERENCES	116
7	APPENDIX I.....	117
7.1	INJECTION TEST DETAILS	117
7.2	WELLTEST INTERPRETATION RESULTS.....	127
7.3	PRODUCTION PERFORMANCE CURVES.....	139
7.4	ECLIPSE RUNS SPECIFICATION	145

List of Tables

Table 2-1	Select stage Bergermeer Storage Specifications.	25
Table 2-2	Reservoir properties DISMID_HIGHKV model (25 layers).	26
Table 2-3	Subsurface realizations LOW, MID, HIGH case, showing permeability multipliers and averages in the gaszone for wells BGM-1 and BGM-7. See section 2.5 for a detailed discussion.	26
Table 2-4	Total GIIP Bergermeer and compartment distribution, model BAG25_ALT2_DISMIDHIGHKV. The two other realizations have the same 'Alt2' fault realization, thus the same GIIP distribution. Note that nevertheless there is significant uncertainty in the volume distribution over the two compartments [1].	26
Table 2-5	Well test interpretation results Bergermeer BGM-1 and BGM-6A. The radius of investigation is of the last build-up. Wells with (*) were previously interpreted by TAQA.	30
Table 2-6	Welltest re-interpretation results BGM-3A and BGM-7 outside the 'sweet spot' area near BGM1. KH values and radius of investigation are given of the last build-ups.	31
Table 2-7	Multiplier values of 'BELL' realizations to create a pessimistic subsurface case. In the 'BELL' realizations, the multiplier has a parabolic profile, in the 'LOG_BELL' realizations the logarithm of the profile is parabolic.	34
Table 3-1	Main lift curve input parameters for vertical and horizontal development wells.	45
Table 3-2	IPR model parameters for horizontal well in Prosper.	45
Table 3-3	Base case values used for well performance sensitivity calculations.	48
Table 3-4	Well performance sensitivity values summary at P _{res} 120 bar and THP 80 bar.	57
Table 4-1	Planned injection scheme [4].	60
Table 4-2	Overview of well test interference results.	68
Table 5-1	Offtake scenarios MID, LARGE, XLARGE field development, based on geological model DISMIDHIGHKV. The LARGE case was taken as the offtake base case, all wells have 7 5/8" Tbg.	76
Table 5-2	Subsurface realizations LOW, MID, HIGH case, showing permeability multipliers and averages in the gas-zone for wells BGM-1 and BGM-7 (see Table 2-1 and section 2.5).	77
Table 5-3	Bergermeer UGS forecast results for Mid, Large and XLarge offtake scenarios, all with DISMIDHIGHKV geological model.	81

Table 5-4	Bergermeer UGS scenarios. Example: The Large scenario is attained with 20 wells, all of 7 5/8" Tbg-size (5 hor. wells BGM-7, 4 hor. wells MAIN and 11 vertical wells) or 16 wells where the vertical wells are of 8 5/8" Tbg-size (5 hor wells Block-II with 7 5/8" Tbg and 11 vertical 9 5/8" in Block-I), or 14 wells where the vertical wells are of 9 5/8" Tbg-size (5 hor wells Block-II with 7 5/8" Tbg and 9 vertical 9 5/8" in Block-I).....	84
Table 5-5	Field performance parameters HIGH CASE, pessimistic horizontal well position (DISMIDHIGHKV_H06_H11)	96
Table 5-6	Field performance parameters BASE CASE, pessimistic horizontal well position (DISMIDHIGHKV_BELL_050_ALT_H06_H11).....	97
Table 5-7	Field performance parameters of LOW CASE, pessimistic horizontal well position (DISMIDHIGHKV_BELL_033_ALT_H06_H11).....	97
Table 5-8	Field performance parameters, high case run sensitivity (DISMIDHIGHKV_H05_H01), optimistic horizontal well position, H05 for MAIN and HOR01 for BGM-7.....	98
Table 5-9	Field performance parameters, high case run sensitivity (DISMIDHIGHKV_H06_H11), pessimistic horizontal well position H06 for MAIN and H11 for BGM-7	98
Table 5-10	Forecast sensitivities summary table	104
Table 5-11	Comparison of 'DISMID_HIGHKV' UGS run with (left) and without (right) local grid refinement.	109
Table 5-12	Bergermeer UGS filling up pressures and volumes.....	112
Table 7-1	Overview of injection rates during Bergermeer injection test 2007.....	117
Table 7-2	Input decks Bergermeer UGS for Performance curves	145
Table 7-3	Input decks Bergermeer UGS without Performance curves	145
Table 7-4	Input decks Bergermeer UGS for faults seen in Summer Injection Test	146
Table 7-5	Input decks Bergermeer UGS drilling sequence and end-of-fieldlife	146
Table 7-6	Well completion data include decks	146
Table 7-7	Includes for production / injection rates of UGS cycles and performance curves	146

List of Figures

Figure 1-1 Location of Bergen concession fields that were part of the History Match study: Bergen (BER), Groet (GRT) and Bergermeer (BGM). The latter field is the main focus of this study. The indicated well positions are at top Rotliegendes reservoir. 19

Figure 1-2 Location of existing BGM wells. Well intersection points plotted are at top Rotliegendes (ROSLU) reservoir. Well BGM4 is a water injector located in a fault block S of the main BGM block and is not connected to the reservoir. Pressures in BGM4 are much higher than in the main BGM block. 20

Figure 2-1 BGM-1 log plot. Tracks indicate (L to R) the perforations, GR, core porosity vs. the PHIE log, DT, core permeability, RT. The porosity log shows the quality deterioration towards the top. Low quality streaks can be identified throughout the section. 23

Figure 2-2 Pressure history of the three fields vs. time. Bergen has seen pressures 50 bars higher than Groet and Bergermeer. Groet pressures have been on either side of Bergermeer pressures, with a maximum pressure difference of ca 35 bars. 24

Figure 2-3 Graph of GWC vs. time as observed in BGM1, 7 and GRT6. The initial contacts for GRT and BGM are assumed to be 2217 and 2227, respectively. 24

Figure 2-4 P/Z plot Bergermeer showing different pressure behaviour for BGM-7 compartment 27

Figure 2-5 Notional faults in the simulation model (Phase 1) based on dynamic information. These are the EW fault across the spillpoint in the north (brown, marked '@ spill'), the extension of Fault 4 west of the BGM7-block (red), and four possible extensions of Fault 2 (green) that separates BGM-7 from BGM-main; 2B alt1, 2, 3 and 4. Fault 2B-'Alt2' was taken for the base case HM. 28

Figure 2-6 Fifth possible fault extension (Alt_5) of the main Fault 2 (Phase 2) plotted on average permeability map in gas zone of 'DISMID_HIGHKV_LOG_BELL_100'. The fault runs straight from BGM-6 and passes west of BGM-3A. Alt_5 is just east of Alt_2, the base case found dynamically in the history matching Phase 1. 28

Figure 2-7 Drawdown vs. gas-rate seen in Bergermeer well tests. Note the huge drawdown difference between BGM3/BGM-7 and the rest of the field due to low permeability and high skin values. 32

Figure 2-8 Plot showing rate-dependant pressure drop in historical well test data. The gradient is an indication of rate-dependant skin; the intercept indicates the mechanical skin value. The BGM-1 test (1979) was used as a reference for rate dependant skin, with a factor 2 higher and 4 lower as sensitivity. 33

Figure 2-9	Roughly SW/NE cross-section through BGM7 (plotted in black). The inferred fault between the BGM7 and BGM-main blocks is also shown (stack of outlined blocks), as is the original GWC. The property plotted is permeability (5-500 mD). The left plot shows a high contrast model (DISMID_HIGHKV_LOG_BELL_100), the right plot a low contrast model (DISMID_HIGHKV).....	35
Figure 2-10	Average permeability maps over the gas zone. Left is the 'DISMID_HIGHKV' model (High Case), average permeability values at BGM7/BGM1 are roughly 300/800 mD. Right shows the 'DISMID_HIGHKV_BELL_050' model (Mid Case), average permeability values at BGM7/BGM1 125/750 mD. The 'BELL_033' run (Low Case) has 2/3 of the 'BELL_050' run (i.e. 85/500 mD).	35
Figure 2-11	Gas zone average permeability map of the 'DISMID_HIGHKV_LOG_BELL_100' realisation on the left (unmatchable). BGM7/BGM1 have permeabilities of ca 20/600 mD. Permeability multiplier used for the 'LOG_BELL_100' case (1 in the middle and 0.03 top/bottom). The wells BGM1 (dark blue) and BGM7 (light blue) are plotted for reference.	36
Figure 2-12	GWC behaviour of BELL_033 (low case) and BELL_050 (mid case) sensitivities. In BGM1, the GWC is 2207 m tvdss at the end of history; BELL_050 and BELL_033 have a GWC of 7, resp. 13 m too shallow due to coning. In BGM-7, the BELL_050 and BELL_033 fit very well at the start, but BELL_033 is much too shallow at the end.	377
Figure 2-13	Pressure match for the BELL_033 alternate. Pressures plotted are the BHP's and the gridblock pressures (9-block average, "WBP9"). For BGM7 the BHP goes to zero, indicating that the historic rates cannot be matched anymore after 2007. Pressures in the main block are somewhat too low, but increasing the fault seal would lower BGM7 pressures (which would make it fail even earlier).	38
Figure 2-14	Left: Late BGM7 history (pressure & rates) showing rates are not met due to BHP limit [BELL_033]. Right: Water production rates for BELL_033.	39
Figure 2-15	Water production (left) and GWC rise (right) for too-pessimistic runs ('BELL_025' and 'LOG_BELL_100'). Historical GWC data give values of about 2207 m at the end of the historic period. It should be noted that the GWC's extracted for BGM7 in the 'LOG_BELL_100' case are somewhat distorted due to the water production.	39
Figure 3-1	IPR plot BGM-1 using isochronal test results of 1979.	41
Figure 3-2	VLP/IPR matching results BGM-1 multirate test-data (1979), MultiRate Jones IPR model and matched VLP parameters	42
Figure 3-3	WDFACCOR match in Eclipse to multi-rate test BGM-1 (1979). The light blue line (WDFACCOR = 1.6e-6) overlays the green line of the previous HM (WDFAC = 2e-5).	44

Figure 3-4	IPR / VLP plot for vertical well model, IPR from well test match BGM-1	46
Figure 3-5	IPR / VLP plot for horizontal well model, IPR model Kuchuk & Goode	46
Figure 3-6	Pressure vs Depth horizontal well model, Pres 120 bar, THP 80 bar	47
Figure 3-7	Pressure vs Depth horizontal well model, Pres 120 bar, THP 40 bar	47
Figure 3-8	Effect of Skin on IPR of vertical well.	48
Figure 3-9	Effect of Skin on IPR horizontal well	49
Figure 3-10	Permeability variations on vertical well IPR model	50
Figure 3-11	Permeability variations on horizontal well IPR model	50
Figure 3-12	CGR sensitivity for vertical wells. The reservoir pressure is 157.5 bar.	51
Figure 3-13	CGR sensitivity for horizontal wells. The reservoir pressure is 120 bar.	52
Figure 3-14	WGR sensitivity for vertical wells. The reservoir pressure is 157.5 bar.....	53
Figure 3-15	WGR sensitivity for horizontal wells. The reservoir pressure is 120 bar.	53
Figure 3-16	Lift curve sensitivity on roughness, Pres 120 bar, THP 80 bar, vertical well.	54
Figure 3-17	Lift curve sensitivity on roughness, Pres 120 bar, THP 80 bar, horizontal well.	55
Figure 3-18	Lift curve sensitivity on tubing size, Pres 120 bar, THP 80 bar, horizontal well.	56
Figure 3-19	Lift curve sensitivity on tubing size, Pres 120 bar, THP 80 bar, vertical well.....	56
Figure 3-20	Tornado plot vertical well performance sensitivities at P _{res} 120 bar and THP 80 bar. Parameter ranges are shown in Table 3-4.	57
Figure 3-21	Tornado plot horizontal well performance sensitivities.	58
Figure 4-1	Predicted pressure behaviour summer injection test, MAIN block volume 13.6 Bcm, BGM-7 block volume 4.0 Bcm, base case model, no aquifer, Qinj 0.75MM sm ³ /d for 3 months in BGM-1, 2 and 6A (total 200 MM sm ³) [Based on 'cont_mid' realization [1].].....	60
Figure 4-2	Zoom-in on the BGM well area, to indicate the relative positions of the wells. The (partly inferred) line between BGM7 and BGM-main blocks is indicated with white lines. The map shows top reservoir, where it is above the original GWC.	62
Figure 4-3	Overview of injection rates and well head pressures of wells BGM-1, BGM-2 and BGM-6 during 2007 Summer Injection Test.....	63
Figure 4-4	BGM-7 BHP before and during summer injection test.....	63
Figure 4-5	BGM-5 BHP before, during and after summer injection test, 1 st run gauge 76760, 2 nd run gauge 76391, 3 rd run gauge 76799.....	64
Figure 4-6	BGM-6 BHP before and during summer injection test.....	64
Figure 4-7	BGM-5 BHP interpretation of injection period interference test, parallel faults.....	66
Figure 4-8	Structural model of Bergermeer as used for well test interpretation, injector at 710 m from observation well BGM-5, left: open compartment with parallel faults, right: closed compartment with non-sealing fault above BGM-6.	67
Figure 4-9	BGM-5 BHP interpretation of shut-in period interference test in closed compartment.	68

Figure 4-10	P/Z plot detrended with initial p/z of 249 bar and GIIP of 16500 Nm3 showing deviation from straight line behaviour. A possible baffle between BGM-3 and BGM-1 could explain higher pressures in BGM-3.....	69
Figure 4-11	BHP pressures in dynamic model summer injection test.....	70
Figure 4-12	Pressure match summer injection test before, during and after injection. Continuous lines are from dynamic model (SUMMERINJ_BFLS4), the dots are field data points	71
Figure 4-13	Baffles in main block as used in history match projected on top Rotliegendes map.....	71
Figure 4-14	Re-history match of Bergermeer production period, with baffles in main compartment as seen in summer injection test. Blue line is new HM, brown line is old HM. Purple diamonds are SBHP values BGM-1, blue diamonds are SBHP values BGM-7.....	72
Figure 4-15	Depth of GWC at 1.1.2007 before start of summer injection test, as forecasted by the dynamic reservoir model	74
Figure 4-16	Depth of GWC as predicted by the dynamic reservoir model over the summer injection test.	75
Figure 4-17	GWC in BGM-1 and BGM-7 during re-HM of production period. The updated dynamic reservoir model (DISMIDHIGHKV_baffles4) has the additional baffles interpreted from the injection test. Note that this model is the high-case model in Table 2-3 and Table 5-2.....	75
Figure 5-1	KH distribution in the BGM field [mDarcy*m]. The data plotted is based on the 'DISMID_HIGHKV_BELL_050' realization. The value is the average permeability over the Rotliegend above the original GWC, multiplied by the distance of the original GWC to the top Rotliegend. (Cf. the very similar plot for the 'CONTMID' realization in [1]). The colour scale used is logarithmic.....	78
Figure 5-2	Location of 25 development wells; 6 horizontals in BGM-7 block, 8 horizontals and 11 verticals in the MAIN block. Length of the horizontal sections is approx. 500m, depths between 2180 and 2210m tvdss. All wells assumed to be drilled from the surface location above BGM-1. The base case forecast (20 wells) uses all 11 verticals and HOR's 1, 2, 4, 5, 6, 8, 11, 12, 13 wells (all with 7 5/8" Tbg).	79
Figure 5-3	Net reservoir height map between top Rotliegend and original GWC at 2227 m (left) and depth of top Rotliegend (colour scale limited to above 2227 m; right)	80
Figure 5-4	Position of dividing fault between Main and BGM-7 compartment (blue) and the baffles in Main, north of BGM-6 (green) and south of BGM-1 (yellow), as discussed in chapter 4. New wells are shown in the left graph, existing wells in the right graph.	80

Figure 5-5	UGS pressure behaviour BGM-7 and Main blocks in old runs, maximum dP 75 bar over the fault, 10-20 cycles needed to equalize the two blocks, model DISMIDHIGHKV.	82
Figure 5-6	UGS pressure behaviour BGM-7 and Main blocks in new runs, maximum dP over the fault 2 bar (DISMIDHIGHKV).	82
Figure 5-7	Forecast result M case (left), total 15 wells, block II: 4 horizontal wells, block I: 11 vertical wells. L case (right), total 20 wells, block II: 5 horizontal wells, block I: 11 vert. and 4 horizontal wells.	83
Figure 5-8	XL case (24 wells). Block II: 6 horizontal wells, block I: 11 vert., 7 horizontal wells.	83
Figure 5-9	GWC movement DISMIDHIGHKV, Medium case, 7 5/8" tbg, 15 wells	85
Figure 5-10	GWC movement DISMIDHIGHKV, Large case, 7 5/8" tbg, 20 wells	85
Figure 5-11	GWC movement DISMIDHIGHKV, Xtra-Large case, 7 5/8" tbg, 24 wells	86
Figure 5-12	GWC maps DISMIDHIGHKV N31, Medium case, 7 5/8" tbg, 15 wells	86
Figure 5-13	GWC maps DISMIDHIGHKV N32, Large case, 7 5/8" tbg, 20 wells.	87
Figure 5-14	GWC maps DISMIDHIGHKV N34, XLarge case, 7 5/8" tbg, 24 wells.	87
Figure 5-15	Forecast sensitivity BELL_050. The Main block (black) and BGM-7 block (red) need time to equilibrate.	88
Figure 5-16	Forecast sensitivity BELL_050. Black is the reservoir pressure in block 2, red is P_res at HOR_01 and green is the P_res at HOR_11. They show that there is internal dP of 25 bar in block-2 at the start of the first cycle and between HOR_01 and HOR_11 dP_res is 10 bar.	89
Figure 5-17	Forecast sensitivity BELL_033. The plot shows equilibration Main and BGM-7 blocks over time.	89
Figure 5-18	Forecast sensitivity BELL_033. The plot shows internal dP of 17 bar in BGM-7 block at start of first cycle.	90
Figure 5-19	GWC swings L758 (20 wells), for mid, high and low subsurface realisations.	90
Figure 5-20	GWC swings BELL_050 model. L758 has 15 wells in MAIN, 5 hor. in block 2 each 3.2 MMm3/d, L858 has 11 vert. in MAIN, 5 hor. in block-2 of 4.4 / 3.2 MMm3/d and XL958 has 11 vert., 6 hor wells of 4.9 / 3.0 MMm3/d. Maximum swings BGM-1 are 13 m, and 10 m in block 2 (BGM-7).	91
Figure 5-21	Comparison of parameterized fits to the Eclipse THP/Rate data. Lines with Darcy term (full) and without Darcy term (dashed) are shown. The bottom plot is a zoom-in of the top plot, showing the difference is small, and only visible at low rates. It should be noted that the fit coefficients in the A=0 case are slightly different from the case where A is used. [The run used is the 'BELL_033_ALT_H06_H11' model, which has lowest permeability.]	93

Figure 5-22	Well production performance plot DISMIDHIGHKV_H06_H11, separate curves for vertical well (MAIN), horizontal well (MAIN) and horizontal well (BGM-7 block).....	94
Figure 5-23	Well injection performance plot DISMIDHIGHKV_BELL_050_ALT_H06_H11, separate curves for vertical well (MAIN), horizontal well (MAIN) and horizontal well (BGM-7 block).....	94
Figure 5-24	Well production performance plot DISMIDHIGHKV_BELL_033_ALT_H06_H11, separate curves for vertical well (MAIN), horizontal well (MAIN) and horizontal well (BGM-7 block).....	95
Figure 5-25	Field performance plots DISMIDHIGHKV_H06_H11 (high case), 20 wells 7 5/8", 5 HOR (BGM-7), 4 HOR (MAIN and 11 VERT (MAIN), at start, halfway at end of injection period.	95
Figure 5-26	Field performance plots DISMIDHIGHKV_BELL_050_ALT_H06_H11 (high case), 20 wells 7 5/8", 5 HOR (BGM-7), 4 HOR (MAIN and 11 VERT (MAIN), at start, halfway at end of injection period.....	96
Figure 5-27	Field performance plots DISMIDHIGHKV_BELL_033_ALT_H06_H11 (low case), 20 wells 7 5/8", 5 HOR (BGM-7), 4 HOR (MAIN and 11 VERT (MAIN), at start, halfway at end of injection period.....	96
Figure 5-28	Pressure difference between UGS 'full' at 145 bar and 'empty' at 95 bar. Run DISMIDHIGHKV_WDF_BFLS4, Large case, 20 wells all 7 5/8". Well shown from north to south are BGM-7, BGM-3A, BGM-6A and BGM-1.	98
Figure 5-29	Spread in well-performance in low subsurface realisation (BELL_033_ALT_H05_H01). The plot displays optimistic performance of wells V_01, H_05 (MAIN) and H01 (BGM-7).	99
Figure 5-30	Spread in well-performance in low subsurface realisation (BELL_033_ALT_H06_H11). The plot displays pessimistic performance of wells V_01, H_06 (MAIN) and H11 (BGM-7).	99
Figure 5-31	Pressure losses in horizontal wells in forecast run DISMIDHIGHKV_H05_H01, (20 wells), HOR_05 in Main (left) and HOR_01 in BGM-7 (right). Dark blue is average reservoir pressure of compartment, green is reservoir pressure of well, red is BHP, light blue is THP.....	100
Figure 5-32	Pressure losses in horizontal wells in forecast run (DISMIDHIGHKV_H06_H11), (20 wells), HOR_06 in Main (left) and HOR_11 in BGM-7 (right). Red is average reservoir pressure of compartment, dark blue is reservoir pressure of well, green is BHP, light blue is THP.....	100
Figure 5-33	Plot of BHP and P_res vs GIP for HOR-5 in Main (left) and HOR-1 in BGM-7 (right). The red curves denote well behaviour (BHP/GIP), the green curves show reservoir-block behaviour (P_reservoir / GIP), model DISMIDHIGHKV_H05_H01.....	101

Figure 5-34	Plot of BHP and P _{res} vs GIP for HOR-6 in Main (left) and HOR-11 in BGM-7 (right). The red curves denote well behaviour (BHP/GIP), the green curves show reservoir-block behaviour ($P_{\text{reservoir}} / \text{GIP}$), model DISMIDHIGHKV_H06_H11.....	101
Figure 5-35	BELL_050 model (mid case subsurface), MAIN block, HOR_06 (left) as used for performance parameters and HOR_04 (right), in southern extreme of the block	102
Figure 5-36	BELL_050 model, BLOCK-2, HOR_11 (left) as used for performance parameters and HOR_12 (right) in north of the block were the reservoir pressure represents the average pressure around the well	102
Figure 5-37	BELL_033 model (low case subsurface), MAIN block, HOR_06 (left) as used for performance curves and HOR_04 (right) in the south of the Main block (not used). Swings in HOR_06 ca 20 bar more than the average, while in HOR_04 it is ca 20 bar less, which indicates that capacity in the south is under-utilised and in the north capacity is 'lost'.	103
Figure 5-38	BELL_033 model, Block-2, HOR11 in the south (left) and HOR_12 in the north (right). The curves show that average reservoir pressure increases with every new cycle. Due to its very low permeability, the production targets are not met in this low case model, while the injection rate is not changed.	103
Figure 5-39	Tornado plot forecast sensitivities vertical well in Main block.....	105
Figure 5-40	Tornado plot forecast sensitivities horizontal well in Main block.....	105
Figure 5-41	Tornado plot forecast sensitivities horizontal well in Block-2.....	106
Figure 5-42	Reservoir pressures, Main, BGM-7 and Groet, leaking fault model, transmissibility multiplied by 100 (0.0002→ 0.02), HM and UGS phase	107
Figure 5-43	Reservoir pressures, Main, BGM-7 and Groet, leaking fault model, transmissibility multiplied by 100 (0.0002→ 0.02), zoom in on UGS phase	108
Figure 5-44	Water contact changes due to grid refinement. In BGM-7 the contact rises, while in BGM-1 (Main) the contact falls with 1-2 m.....	109
Figure 5-45	Plot of pressure (GAS_POTN) gradients at the end of HM (plot is @ 1-May-1996); the shape of the contours shows that in the LGR grid, the pressure gradient-size is ample @ 0.2 bar	110
Figure 5-46	Plot of pressure gradients during the UGS injection phase, the Main block includes a LGR for the 'sweet spot' with the vertical wells. The gradient size in the LGR is ca 2 bar.	110
Figure 5-47	Plot of pressure gradients during the UGS injection phase, the BGM-7 block does not have LGR. The gradient size of ca 8 bar in BGM-7 is well captured by the original gridblock-size.....	111
Figure 5-48	Reservoir pressures of optimal drilling sequence, 5 cycles and end-of-fieldlife modelled in Eclipse.	112

Figure 5-49	End-of-fieldlife model (Eclipse), gas-rates per compartment for base case forecast (20 wells, 7 5/8" tbg).....	113
Figure 7-1	BGM-6 plot of interpreted fall-off period.....	118
Figure 7-2	BGM-6 log-log plot of fall-off period.....	118
Figure 7-3	Main results BGM-6 fall-off test.....	119
Figure 7-4	BGM-5 interpretation injection period after 2 nd gauge retrieval, well distance 750.....	120
Figure 7-5	BGM-5 interpretation injection period after 2 nd gauge retrieval, well distance 500m.....	121
Figure 7-6	BGM-5 interpretation injection period after 3 rd gauge retrieval, well distance 710m, parallel faults.....	122
Figure 7-7	Semi-log BGM-5 interpretation injection period after 3 rd gauge retrieval.....	123
Figure 7-8	Log-log BGM-5 interpretation injection period after 3 rd gauge retrieval, results KH 17400 mD*m, k 132 mD, phi 21.7%.....	124
Figure 7-9	BGM-5 interpretation shut-in period after 3 rd gauge retrieval, closed compartment.....	125
Figure 7-10	Semi-log plot BGM-5 shut-in period after 3 rd gauge retrieval, closed compartment.....	126
Figure 7-11	BGM1 1986, partial penetration model, log-log plot build-ups.....	127
Figure 7-12	BGM-1, 1987, partial penetration model, log-log plot build-ups.....	128
Figure 7-13	BGM-1, 1990, partial penetration model, log-log plot build-ups.....	129
Figure 7-14	BGM-1, 1997, partial penetration model, log-log plot build-ups.....	130
Figure 7-15	BGM-3A, 1988, partial penetration model, log-log plot build-ups.....	131
Figure 7-16	BGM-3A, 1990, partial penetration model, log-log plot build-ups.....	132
Figure 7-17	BGM-6A, 1987, vertical homogeneous model, log-log plot build-ups.....	133
Figure 7-18	BGM-7, 1990, vertical homogeneous model, log-log plot build-ups.....	134
Figure 7-19	BGM-7, 1990, vertical homogeneous model, log-log plot and semi-log results drawdowns.....	135
Figure 7-20	BGM-7, 1994, vertical homogeneous model, log-log plot build-ups.....	136
Figure 7-21	BGM-7, 1994, vertical homogeneous model, log-log plot drawdowns.....	137
Figure 7-22	BGM-7, 1997, vertical homogeneous model, log-log plot build-ups.....	138
Figure 7-23	Field performance low case (BELL_033_ALT_H06_H11), Large offtake (20 wells).....	139
Figure 7-24	Field performance mid case (BELL_050_ ALT_H06_H11), Large offtake (20 wells).....	139
Figure 7-25	Field performance high case (DISMIDHIGHKV_H06_H11), Large offtake (20 wells).....	140
Figure 7-26	Well production performance low case (BELL_033_H06_H11), , 7 5/8" Tbg's.....	140
Figure 7-27	Well injection performance low case (BELL_033_H06_H11), , 7 5/8" Tbg's.....	141

Figure 7-28	Well production performance mid case (BELL_050_H06_H11), 7 5/8" Tbg's.....	141
Figure 7-29	Well injection performance mid case (BELL_050_H06_H11), 7 5/8" Tbg's.	142
Figure 7-30	Well production performance high pessimistic case (DISMIDHIGHKV_H06_H11), 7 5/8" Tbg's.	142
Figure 7-31	Well injection performance high pessimistic case (DISMIDHIGHKV_H06_H11), 7 5/8" Tbg's.	143
Figure 7-32	Well production performance high optimistic case (DISMIDHIGHKV), 7 5/8" Tbg's.....	143
Figure 7-33	Well injection performance high optimistic case (DISMIDHIGHKV), 7 5/8" Tbg's.....	144

Executive Summary

The present report documents a 2nd phase of work on the sub-surface model of the Bergermeer field. This depleted gas field is scheduled for conversion to a UGS. In the first phase the model was history matched, both w.r.t. pressure behavior and gas-water contact dynamics. The present work is focused on forecasting the behavior of the field when converted to a UGS. To this end several subsurface realizations are carried forward, and combined with several surface/development scenarios.

During the summer of 2007 an injection test was executed in the Bergermeer field. This test has been interpreted. The test highlighted that at the timescales of UGS operation the pressure behavior of the field may be more complicated than is evidenced by the production history. On the basis of this test some modifications were made to the subsurface model realizations. Additionally, well hydraulic modeling has been carried out. This, in combination with the updated subsurface model realizations, was used to generate capacity curves for the prospective Bergermeer UGS under various UGS conditions.

The main reservoir uncertainty thus identified is the lack of definition outside the main reservoir area in the SE of the field, towards the North and in particular in the western compartment (which contains the BGM-7 well). The compartment volume is uncertain due to the unknown position of the main dividing fault; the reservoir quality is uncertain due to insufficient depth control of the top Rotliegend horizon. It is expected that five horizontal wells need to be placed in this block in the UGS phase. The wells are needed to limit the pressure differential over the main fault, which has earlier proved to be non-sealing. Continuous monitoring of the downhole pressures after the 2007 injection test is recommended in order to confirm the transmissibility of the non-sealing fault.

The uncertainty towards the North of the field, and the inability to put wells there from the surface facilities near BGM-1, poses the risk of a more adverse cushion gas/working gas ratio.

A further uncertainty is introduced by the remaining friction between well test permeabilities and history match permeabilities: the former cover a lower range than the latter, which are constrained by the contact match in particular. After further, detailed, interpretation of the pressure transients, the two ranges do appear to overlap somewhat. The permeability uncertainty is captured by testing the UGS against multiple subsurface realizations, spanning the range from well test permeabilities to history match permeabilities.

For future planning purposes it is recommended to set up one (or multiple, to capture uncertainty) material balance model (MBAL), calibrate it to dynamic modeling results and link it to well outflow models (Prosper). As the key elements of the subsurface behavior are relatively simple, this will reduce effort while maintaining quality.

1 Introduction

The Bergermeer gas field is part of the onshore Bergen concession. The field has produced since 1971, from a gas accumulation of about 17 BNm³ originally in place, which is divided in two communicating compartments. It is nearing the end of its field life, and is currently considered for conversion to underground gas storage (UGS) facility. A map of the field and its neighbors is shown in Figure 1-1.

During the first half of 2007, a modeling study, commissioned by Taqa Energy BV (formerly BP Netherlands), was executed. In the first phase of this study [1] a subsurface model for the field was built. This model was history matched, and some first steps were done to assess the behavior of the field under UGS conditions. In addition, the possibility of communication between the Bergermeer field (BGM) and its neighbors Groet (GRT) and Bergen (BER) was studied, as well as the reason for and impact of the water contact rise observed in Bergermeer (and Groet).

The present report discusses the follow up work. In this work the UGS behaviour was examined in more detail. It was assessed how the subsurface uncertainties compare to well & other uncertainties. In addition, the injection test that took place during the summer of 2007 was interpreted, and its findings were incorporated.

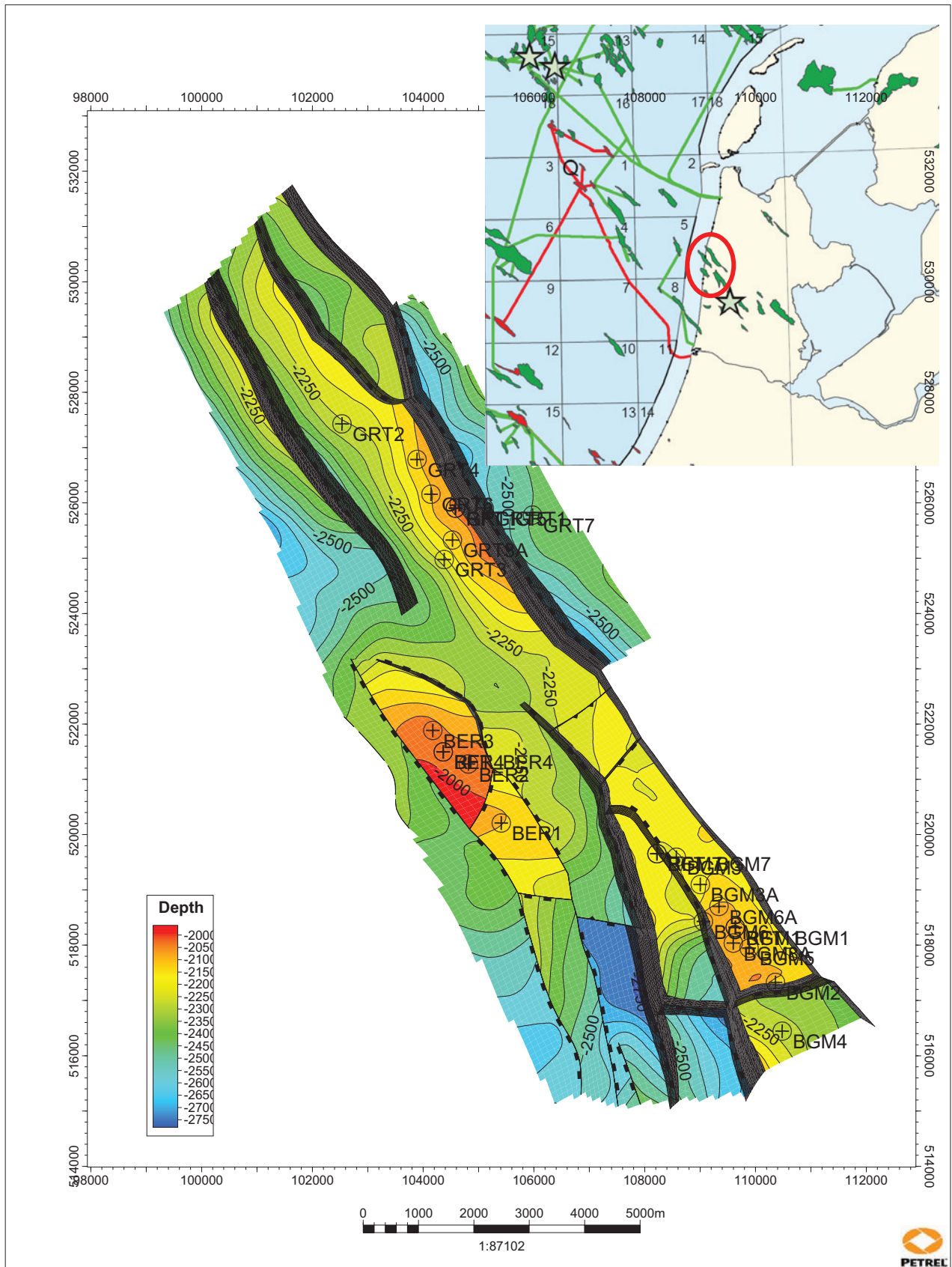


Figure 1-1 Location of Bergen concession fields that were part of the History Match study: Bergen (BER), Groet (GRT) and Bergermeer (BGM). The latter field is the main focus of this study. The indicated well positions are at top Rotliegendes reservoir.

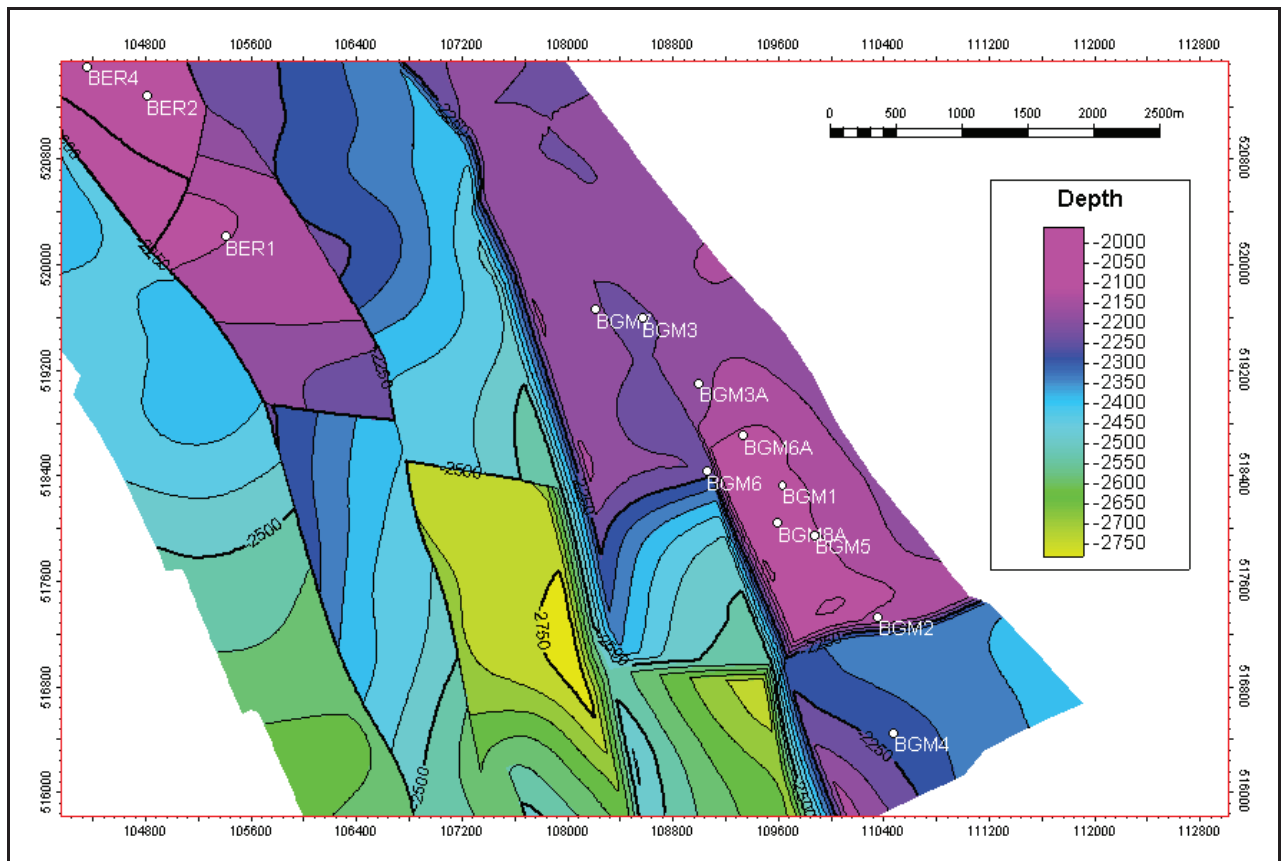


Figure 1-2 Location of existing BGM wells. Well intersection points plotted are at top Rotliegendes (ROSLU) reservoir. Well BGM4 is a water injector located in a fault block S of the main BGM block and is not connected to the reservoir. Pressures in BGM4 are much higher than in the main BGM block.

2 UGS Inputs

2.1 Phase 1 Findings & Model description

A detailed description of the Bergermeer field and model is contained in the report for the first phase of this study [1] and will not be repeated here. We repeat only the main points here.

The model constructed is a 3D Petrel model of the Rotliegend layer, incorporating Bergermeer (BGM), Groet (GRT) and Bergen (BER), as well as some water-bearing blocks in the surroundings. Input to the model were well logs & seismic surfaces as provided by Taqa. Several top surfaces were used (as sensitivities) to capture the Time/Depth conversion uncertainty. In addition, a range of property models was generated to capture the possible range of heterogeneity seen in the wells. These heterogeneities are twofold (Figure 2-1): firstly there is a large scale (>10 m) deterioration of the sand quality upwards, and downwards, resulting in a 'bell shape' porosity and permeability profile. Secondly, there are smaller scale heterogeneities in which the properties are locally much worse. The former kind is continuous with a high degree of certainty and probably diagenesis-related (the upward deterioration reflects a cementation gradient). The second kind is of unclear origin (the cores were rather poorly preserved), the extent of these features was therefore varied.

The 3D model contains only faults that could be interpreted on seismic. As regards the BGM field proper, the production data clearly shows that there are (at least) two compartments: the well BGM7 shows higher pressures than the other wells (Figure 2-4; accordingly the compartments are referred to as 'MAIN' and 'BGM7'). The fault between the two compartments is not fully visible on seismic. Sensitivities have been run on the various possibilities for its northwards extension. The best fit with the dynamic data was obtained with a northeastwards extension of the fault.

Base case volumetrics were fixed using a material balance study. It should be noted that the static volumes for BGM had to be multiplied by 1.1 to 1.2 to obtain a material balance match. A likely suspect for the cause of this problem is the top surface: the Time/Depth conversion uncertainty exceeds this amount.

A dynamic model (for Eclipse100) was generated directly from the Petrel model. The fields were (in combination) history matched on pressure behavior as well as water contact rise. Where relevant, water breakthroughs were used to constrain it.

The most important conclusions of the first phase study were:

- The material balance (p/z) of the reservoirs shows that there is little or no communication between Bergermeer, Bergen and Groet.
- Similarly, the material balance shows the fields to have little or no aquifer.
- The main uncertainty from the history match concerns the relative sizes of the two compartments of the Bergermeer field, and the nature of the baffle separating them.
- The observed contact rises in Bergermeer and (to some extent, depending on the interpretation of the most recent observation) Groet can be explained well; the simulations show the contact is likely not flat. Observations of the GWC in other wells than BGM1, most notably BGM7, could test

this prediction.

- The well tests, in combination with the contact rise, fix the horizontal and vertical permeability reasonably well: horizontal permeabilities are of the order of 500 mD, with k_v/k_h not far from 1. Some uncertainty on the overall permeability level remains, related to the fact that there is certainly a permeability profile over the reservoir zone, of which the well tests only show an average. Moreover, the well test analyses are not clean fits. Nevertheless, high k_v/k_h values would indicate that the heterogeneities seen in the logs have horizontal length scales less than 100m. [The well-tests are revisited further on in this report.]
- There appears little risk of subsurface gas losses out of the Bergermeer field across the spill point to Groet or Bergen; the field as a whole is expected to show fairly simple, tank-like, behavior (even if we would assume, contrary to well test evidence, the heterogeneities to be continuous and prominent, and k_v/k_h to be low). However, there are some complexities in the interaction between the two Bergermeer compartments. In particular the contact movements in the smaller compartment (around well BGM7) can be quite large.

Regarding the first conclusion, it should be noted that the study did not incorporate models with non-linear fault seal (i.e. where the fault seal depends on pressure difference). The simulator used (Eclipse 100) allows fault models where the fault is closed below a certain pressure differential, and opens up above it. This simplistic model does not offer a better fit to the pressure data. However, the historical pressure difference between the fields/compartments is limited, so that the history match strictly speaking does not allow one to draw conclusions if pressure differentials exceed this amount.

As mentioned earlier, the relative volume of the two BGM compartments is an issue. In the material balance modeling, the volume in the BGM-7 block could be varied between 2 and 7 Bscm while still attaining a reasonable match ([1]). However, cases with smaller volumes for BGM7 overestimate the early historical pressure drop observed in this well. Therefore volumes towards the higher end of this range for the BGM7 compartment are preferred, but these cannot be justified on the basis of the static model. It was hoped that the BGM summer injection test could shed some light on this volume distribution issue, in addition to determining the injectivity of the reservoir and constraining the fault transmissibilities.

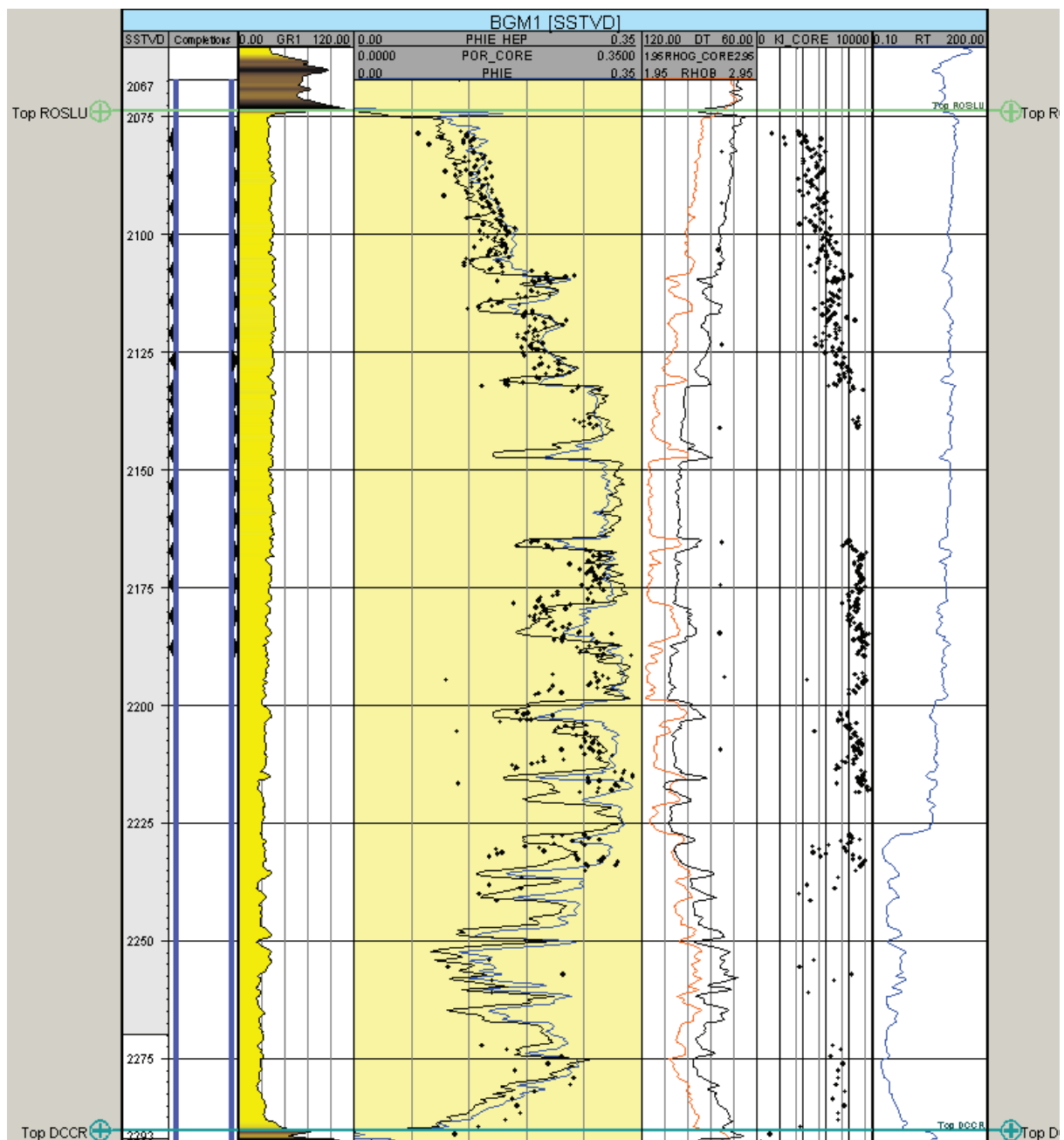


Figure 2-1 BGM-1 log plot. Tracks indicate (L to R) the perforations, GR, core porosity vs. the PHIE log, DT, core permeability, RT. The porosity log shows the quality deterioration towards the top. Low quality streaks can be identified throughout the section.

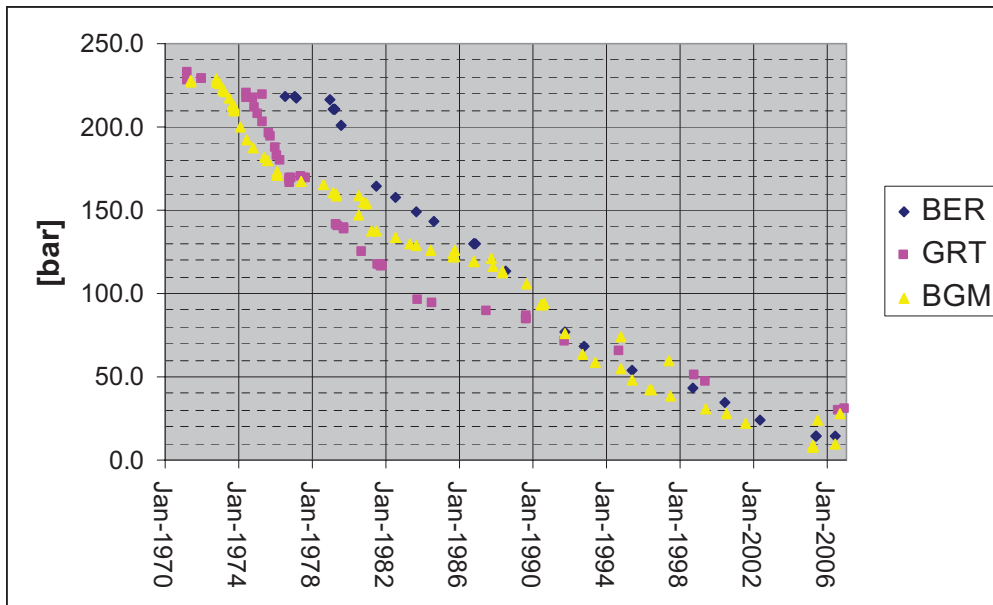


Figure 2-2 Pressure history of the three fields vs. time. Bergen has seen pressures 50 bars higher than Groet and Bergermeer. Groet pressures have been on either side of Bergermeer pressures, with a maximum pressure difference of ca 35 bars.

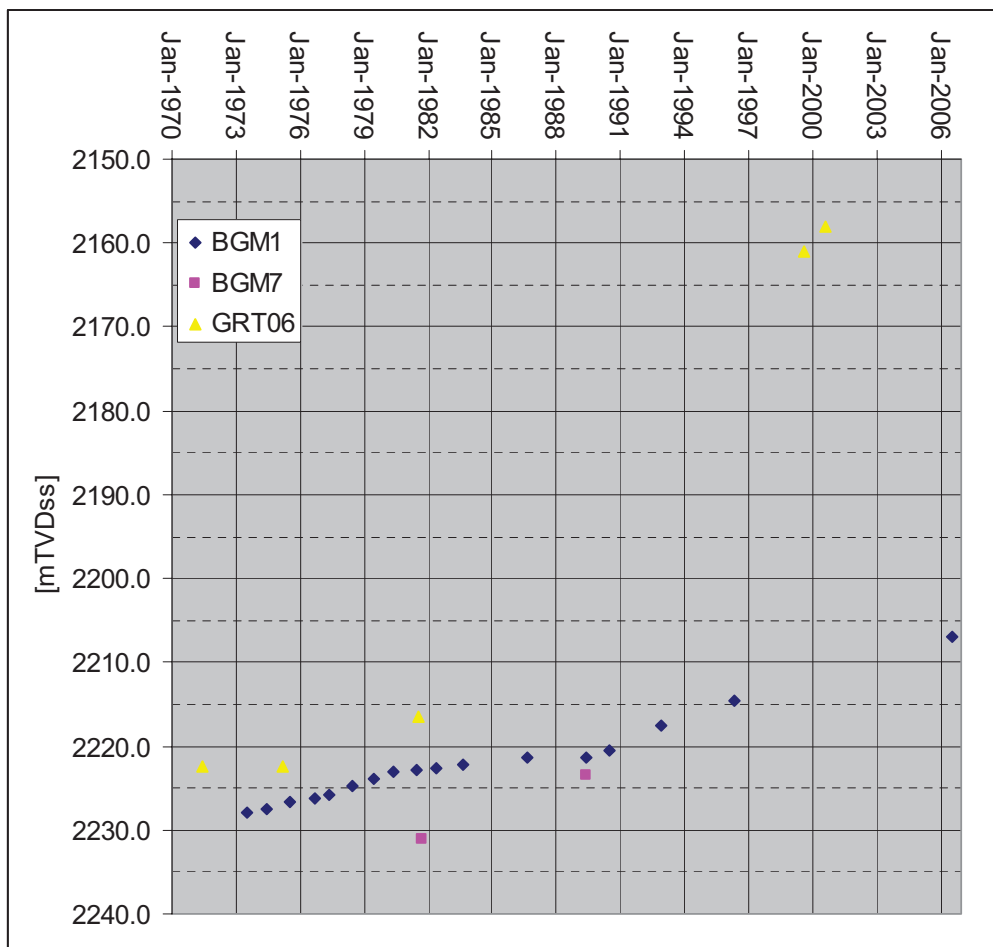


Figure 2-3 Graph of GWC vs. time as observed in BGM1, 7 and GRT6. The initial contacts for GRT and BGM are assumed to be 2217 and 2227, respectively.

2.2 UGS Storage Specifications

[deleted text because of confidentiality]

Table 2-1 Select stage Bergermeer Storage Specifications.

Detailed well performance modelling was carried out to better quantify the expected pressure losses in the tubing at the expected high rates.

2.3 Subsurface Model & Realizations

For the present phase of the study the model from the previous phase was re-used. As will be discussed later, interpretation of the summer injection test has confirmed the choice for the 'DISMID_HIGHKV' (or 'DISCONT_MID_HIGHKV') model to be the most likely model for Bergermeer. As discussed in [1], this model has the least extensive low-porosity streaks. Also the average horizontal permeability is somewhat lower than in the other models, but it has substantially higher vertical permeabilities. The model parameters as used for the UGS are summarized below in Table 2-2. It should be noted that the properties are *overall* averages for the model. The model has (roughly) 92000 active gridblocks of 100x100x10 m size. A model-variant with local grid refinements was run to check the effect of well-interference in the forecast results (section 5.7.4.).

Porosity [%]	Permeability (Kh) [mD]	Kv / Kh	Avg. width low-perm. streaks [m]
19.7	601	0.502	250

Table 2-2 Reservoir properties DISMID_HIGHKV model (25 layers).

In a later stage it was found that the DISMIDHIGHKV model resulted in too optimistic results when compared to well tests, especially from the low productivity wells BGM-7 and BGM-3A in the north and west of the field (see Welltests section 2.4 and HM-chapter 2.5). Some permeability adjustments on the BGM gas zone were therefore done in order to define different subsurface realizations for LOW, MID and HIGH case forecast, see Table 2-3. A map of the average permeability in the gas-zone is given by Figure 2-10 (High Case) and Figure 2-11 (left graph shows Mid Case). The subsurface realizations have relatively low rock compressibility and no aquifer, as detailed in [1]. The impact of subsurface models on results is found in the forecasts sensitivity section 5.5.

Case	Name	PERM MULTX (top-mid)	Perm.av. BGM-7	Perm.BGM-1
LOW	DISMIDHIGHKV_BELL_03 3	0.17 – 0.67	85	500
MID	DISMIDHIGHKV_BELL_05 0	0.25 – 1.00	125	750
HIGH	DISMIDHIGHKV	1.00 – 1.00	300	800

Table 2-3 Subsurface realizations LOW, MID, HIGH case, showing permeability multipliers and averages in the gaszone for wells BGM-1 and BGM-7. See section 2.5 for a detailed discussion.

BERGERMEER TOTAL [BSm3]	MAIN [BSm3]	BGM-7 [BSm3]
17.61	13.61	4.00

Table 2-4 Total GIIP Bergermeer and compartment distribution, model BAG25_ALT2_DISMIDHIGHKV. The two other realizations have the same 'Alt2' fault realization, thus the same GIIP distribution. Note that nevertheless there is significant uncertainty in the volume distribution over the two compartments [1].

The distribution of the gas volumes initially-in-place according to fault realization 'Alt2' is given in Table 2-4. Note that the total volume of 17.61 BSm3 was determined during the history matching process in the previous phase. Dividing the above GIIP by 1.055, the GIIP is 16.7 in BNm3 (Total), 12.9 BNm3 (Main) and 3.8 BNm3 (BGM-7). A pore-volume multiplier of 1.19 (+19%) was used on the Bergermeer geological model. This indicates that the dynamically connected volume is bigger than what can be interpreted from seismic. This can be caused a.o. by a difference in the top map of the Rotliegend or by a difference in

location of the bounding faults [1]. The historical data is insufficiently constraining to determine the nature or location of the discrepancy with any certainty.

The Bergermeer P/Z plot (Figure 2-4) shows the different pressure-behavior of BGM-7 compared to the other wells. It indicates that the fault seen in seismic splits the field in 2 blocks. History matching of the field in the previous phase indicated that the fault is semi-permeable. The maximum pressure difference over the fault of ca 20 bar was reached in the 90's.

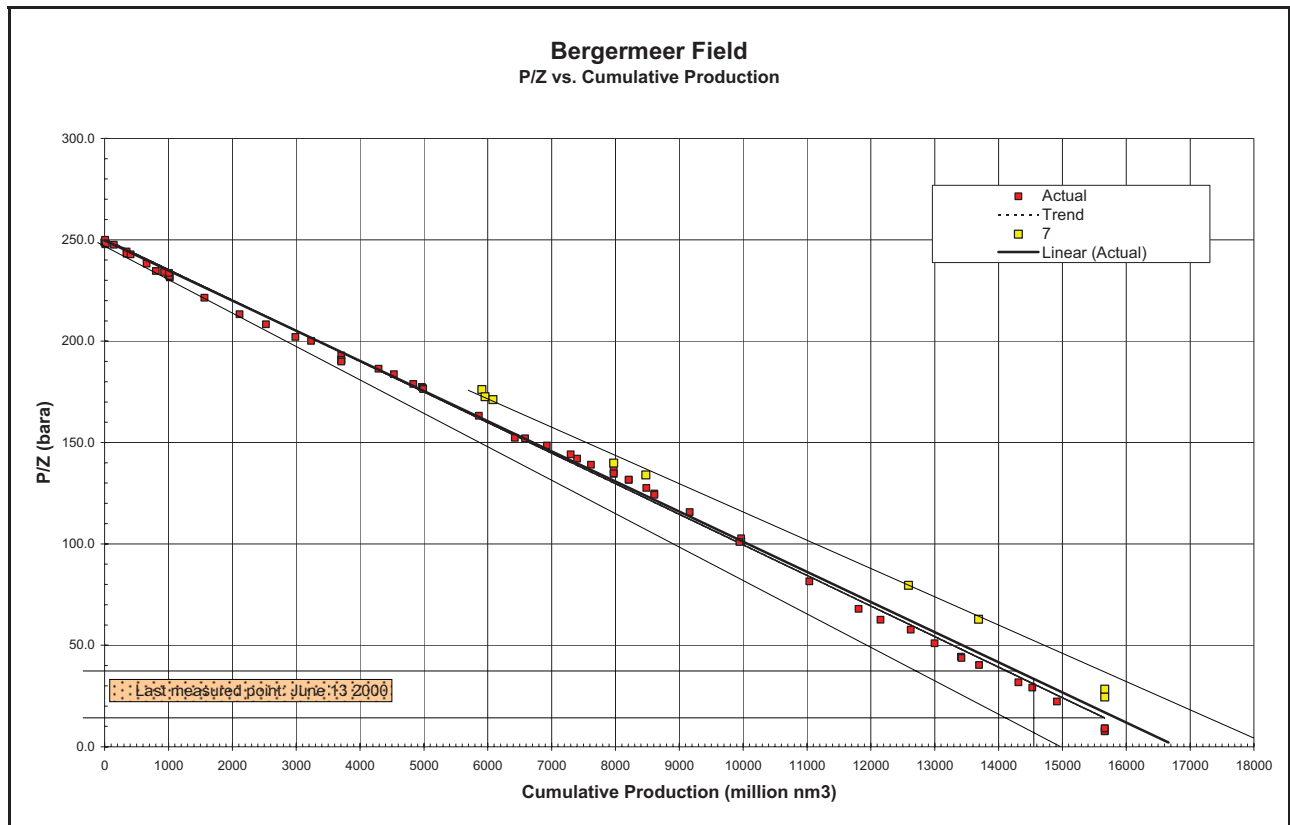


Figure 2-4 P/Z plot Bergermeer showing different pressure behaviour for BGM-7 compartment

As discussed above in section 2.1 (Phase 1 Findings & Model description), there were several realizations for the extension of the fault between MAIN and BGM7 beyond the part visible on seismic. The most western extension of fault 2B was realization 'Alt1', the eastwards extension was 'Alt4' while the base case HM was based on the north-eastwards extension called 'Alt2', see Figure 2-5. This latter variant, 'Alt2', gave the best match and was used for the work in this 2nd phase of the study. The distribution of the gas volumes initially-in-place according to fault realization 'Alt2' is given in Table 2-4.

While making maps for this Phase 2 report, a tentative fifth alternative extension of the Main fault (Alt_5) was identified, see Figure 2-6. The fault runs straight from BGM-6 and passes west of BGM-3A, leaving both BGM-7 and BGM-3 in Block 2. Alt_5 is just east of Alt_2, the base case found dynamically in the history matching Phase 1. Compared to the previous phase's model, the present models have two

additional baffles in the main block as a result of the interpretation of the injection test carried out over the summer of 2007 (chapter 4).

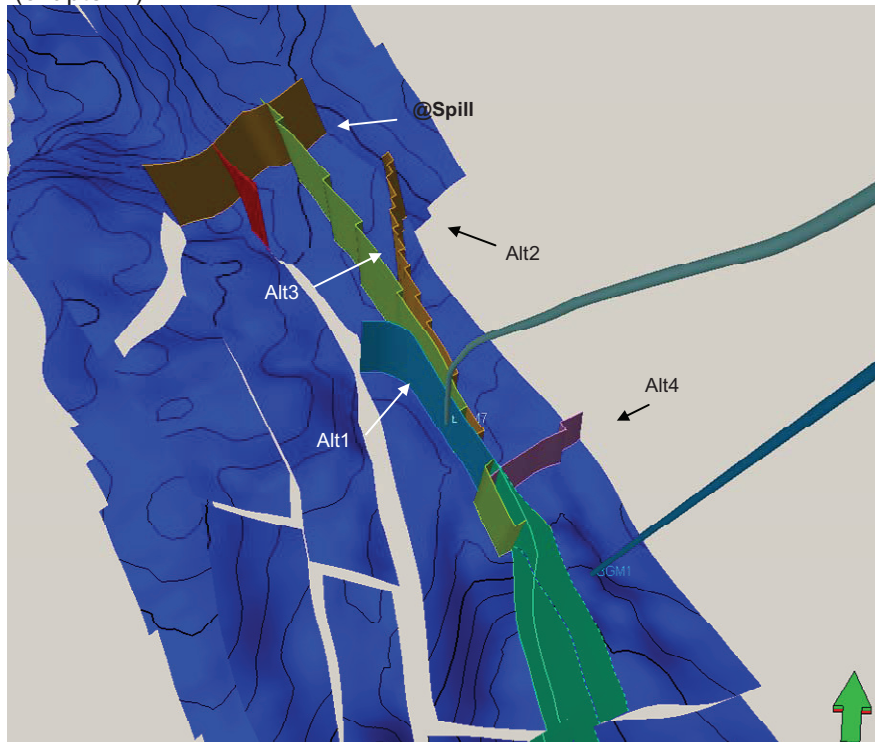


Figure 2-5 Notional faults in the simulation model (Phase 1) based on dynamic information. These are the EW fault across the spillpoint in the north (brown, marked '@ spill'), the extension of Fault 4 west of the BGM7-block (red), and four possible extensions of Fault 2 (green) that separates BGM-7 from BGM-main; 2B alt1, 2, 3 and 4. Fault 2B-'Alt2' was taken for the base case HM.

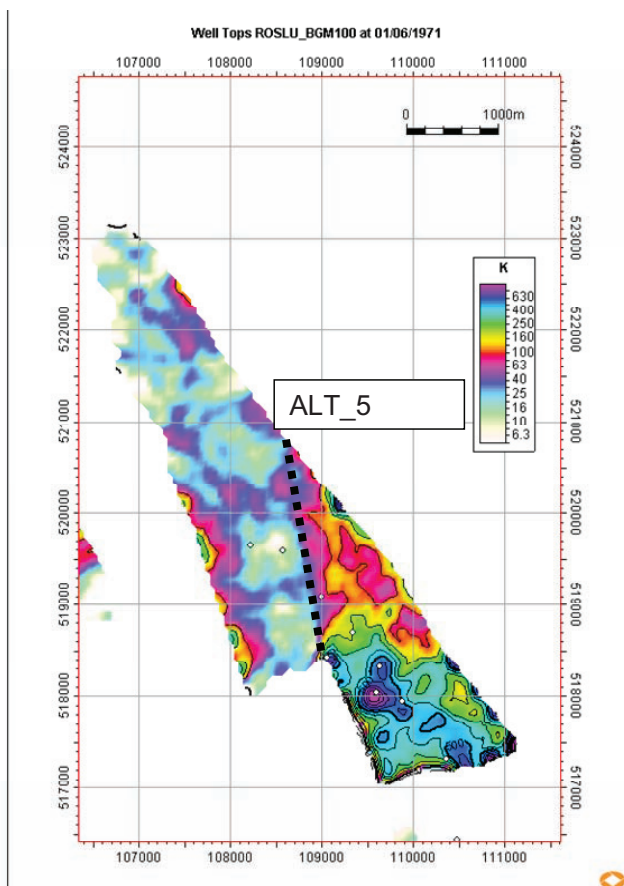


Figure 2-6 Fifth possible fault extension (Alt_5) of the main Fault 2 (Phase 2) plotted on average permeability map in gas zone of 'DISMID_HIGHKV_LOG_BELL_100'. The fault runs straight from BGM-6 and passes west of BGM-3A. Alt_5 is just east of Alt_2, the base case found dynamically in the history matching Phase 1.

The PVT data was given in section 5.1.1 [1] of the previous modelling-phase. This was used for this phase of the study. Effects of the different composition of the injection gas were neglected.

No PVT sample data for condensate ratios was available (either historically, or for the UGS phase). Subsurface flow effects of the condensate have been neglected.

Details on special core analysis and relative permeability parameters used in this phase are found in section 5.1.2 [1] of the previous modelling report.

2.4 Well Test Data

A significant amount of well test data is available for Bergermeer. Most well tests were isochronal (multi-rate) tests, with the purpose of determining the deliverability of the well. The typical test-sequence consisted of ca 4 flowing and build-up periods of equal duration, sometimes ended by a longer flowing and build-up period. Much of the data consists of interpretation results, in paper or digital format. Some of the data also includes the raw pressure and rate data, and from one well test, both the rates, FTHP and FBHP data could be found. Some well tests were re-analyzed in the previous phase (section 5.1.5 of the previous report [1]). As the friction between the well test results and the history match constraints on permeability became more pressing during the present phase of the project, additional well test pressure transient interpretations were done in this phase to attempt to resolve some of the remaining questions regarding rate-dependant skin as well as reservoir permeability.

BGM-1

The four tests that were re-analyzed indicate that although the perforation length was increased from 17 to 117 m, the productivity (KH) appears to have stayed about the same. This indicates that the same reservoir-section contributes to flow throughout. The net reservoir height of ca 110 m was previously taken to calculate a permeability of ca 400-600 mD. This is different from the log-derived permeability of ca 1-2 Darcy. It is however arguable if the total net section is seen by the tests. The core-based log- permeability in the upper reservoir section is only a fraction of that seen in the center Rotliegend section (Figure 2-1), also the continuity and transmissibility of the low quality streaks in the Rotliegend is unknown. If the well tests KH is discounted for the poor upper reservoir zone, the permeability could increase to ca 1 Darcy.

The non-Darcy skin from the 1979 test in BGM-1 was taken as a reference for the dynamic model. Like the 1986 test, it has only 17 m perforated. A non-Darcy skin value of 49 per MMm³/d was derived by comparing it to the 1986-test (dSdQ of 32/MMm³/d), see Figure 2-8 and Table 2-5. This is very large. It has decreased to 17 per Mm³/d in 1997 after reperforation. Still, this non-Darcy skin value is considered too high for future wells as they will have a larger wellbore radius and OH-completion, thus drastically reducing downhole velocities.

It is recommended to run a PLT during a next well test of BGM-1 in order to see the contributing layers.

BGM-6

The 1987 tests was difficult to match with a partial penetration model of 60 m perms over 120 meter net reservoir. This resulted in skins of ca. -5. The skin could be decreased to -3 with a homogeneous vertical well model. The drawdown from the 2007 summer injection tests has a somewhat higher permeability value while the skin value is lower, see Table 2-5.

[deleted text because of confidentiality]

Well	Date	Perforation Length [m]	KH [mD*m]	Skin (mech.)	dS/dQ [MMm ³ /d] ⁻¹	Rinv [m]
BGM1	XXX	XXX	XXX	XXX	XXX	XXX
BGM1	XXX	XXX	XXX	XXX	XXX	XXX
BGM1	XXX	XXX	XXX	XXX	XXX	XXX
BGM1*	XXX	XXX	XXX	XXX	XXX	XXX
BGM1	XXX	XXX	XXX	XXX	XXX	XXX
BGM2*	XXX	XXX	XXX	XXX	XXX	XXX
BGM5*	XXX	XXX	XXX	XXX	XXX	XXX
BGM5*	XXX	XXX	XXX	XXX	XXX	XXX
BGM6	XXX	XXX	XXX	XXX	XXX	XXX
BGM6*	XXX	XXX	XXX	XXX	XXX	XXX
BGM6*	XXX	XXX	XXX	XXX	XXX	XXX
BGM6*	XXX	XXX	XXX	XXX	XXX	XXX
BGM6	XXX	XXX	XXX	XXX	XXX	XXX
BGM8*	XXX	XXX	XXX	XXX	XXX	XXX

Table 2-5 Well test interpretation results Bergermeer BGM-1 and BGM-6A. The radius of investigation is of the last build-up. Wells with (*) were previously interpreted by TAQA.

BGM-3A

Table 2-6 presents well test interpretation results from BGM-3A and BGM-7. Both wells are located outside the ‘sweet spot’ area, and have consequently less reservoir height and quality. BGM-3A is interpreted with partial penetration model, where only 10 out of 30 m net reservoir contributes to flow. The permeability is therefore estimated at ca 100 mD. The skin values are very high, mechanical skin of 13 to 18, the geometric skin of 9, and a very high non-Darcy skin of 70 per MMm³/d. If possible, a reperforation of the 1972 perms (2 spf) could lower skin dramatically.

It should be noted that the BGM-3A well is the only well in the project without logs. This means that the properties in the Eclipse model are not constrained those observed in the well. The discrepancy between the well performance and the properties in the model in that location is probably partly caused by this. A contributory cause is likely the fact that the DISMID model underestimates the ‘bell’ permeability profile

away from well control, as already observed in the previous study [1]. To counter this, the ‘BELL’ realizations were created (Table 2-3). Nevertheless, it can serve as a caveat on the ability of the model to predict reservoir properties away from well control.

BGM-7

BGM7 is the only well that, from its historical pressure behaviour, can be identified to be in a different compartment than the other wells. The tests were interpreted with vertical homogeneous, double porosity or composite models. It was impossible to match both drawdowns and build-ups at the same time. In the 1990 test, the KH calculated from the build-ups is a factor 10 lower than the drawdown. The 1994 test shows that the KH is dependant of the flow-rate, the larger the flow-rate, the larger the KH. The 1997 test has KH in the DD which is ca 2 to 3 times the KH in the BU’s. This discrepancy could be explained by the presence of horizontal boundaries and high permeable layers below the perforations. As the pressure difference over the horizontal boundary is greater than the breakthrough pressure during the drawdown than less during the build-up, the KH thus increases during the DD’s and decreases in the build-ups.

The contributing reservoir-height during the Build-ups is probably not more than 10 meter, thus calculating a permeability of 20 to 40 mD over the perms, and a permeability of 40 to 100mD over the net reservoir-section from the drawdowns.

An overview of the well test re-interpretation using Kappa is given in the Appendix 7.2.

[deleted text because of confidentiality]

Well	Date	Perf. Length [m]	KH [mD* m]	Skin (mech.)	dS/dQ [MMm ³ /d] ⁻¹	Rinv [m]
BGM-3A	XXX	XXX	XXX	XXX	XXX	XXX
BGM-3A	XXX	XXX	XXX	XXX	XXX	XXX
BGM-7	XXX	XXX	XXX	XXX	XXX	XXX
BGM-7	XXX	XXX	XXX	XXX	XXX	XXX
BGM-7	XXX	XXX	XXX	XXX	XXX	XXX

Table 2-6 Welltest re-interpretation results BGM-3A and BGM-7 outside the ‘sweet spot’ area near BGM1. KH values and radius of investigation are given of the last build-ups.

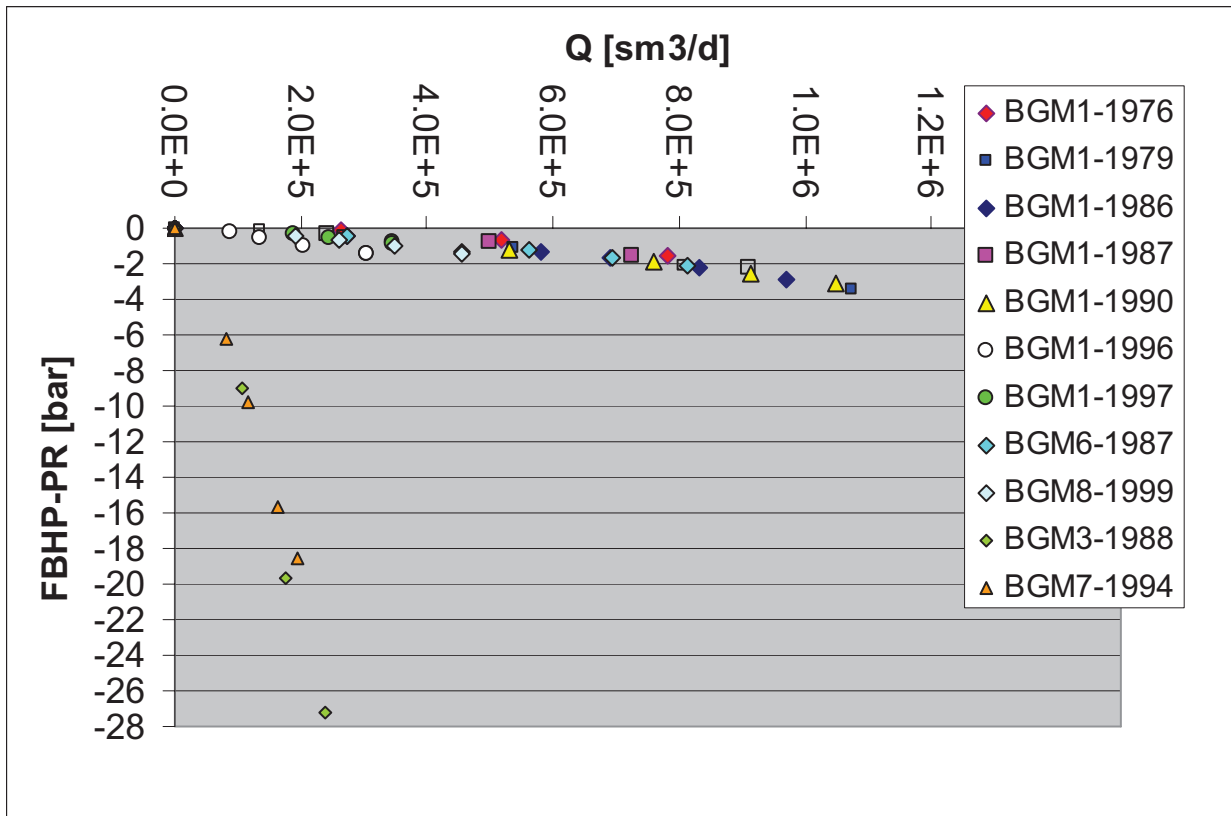


Figure 2-7 Drawdown vs. gas-rate seen in Bergermeer well tests. Note the huge drawdown difference between BGM3/BGM-7 and the rest of the field due to low permeability and high skin values.

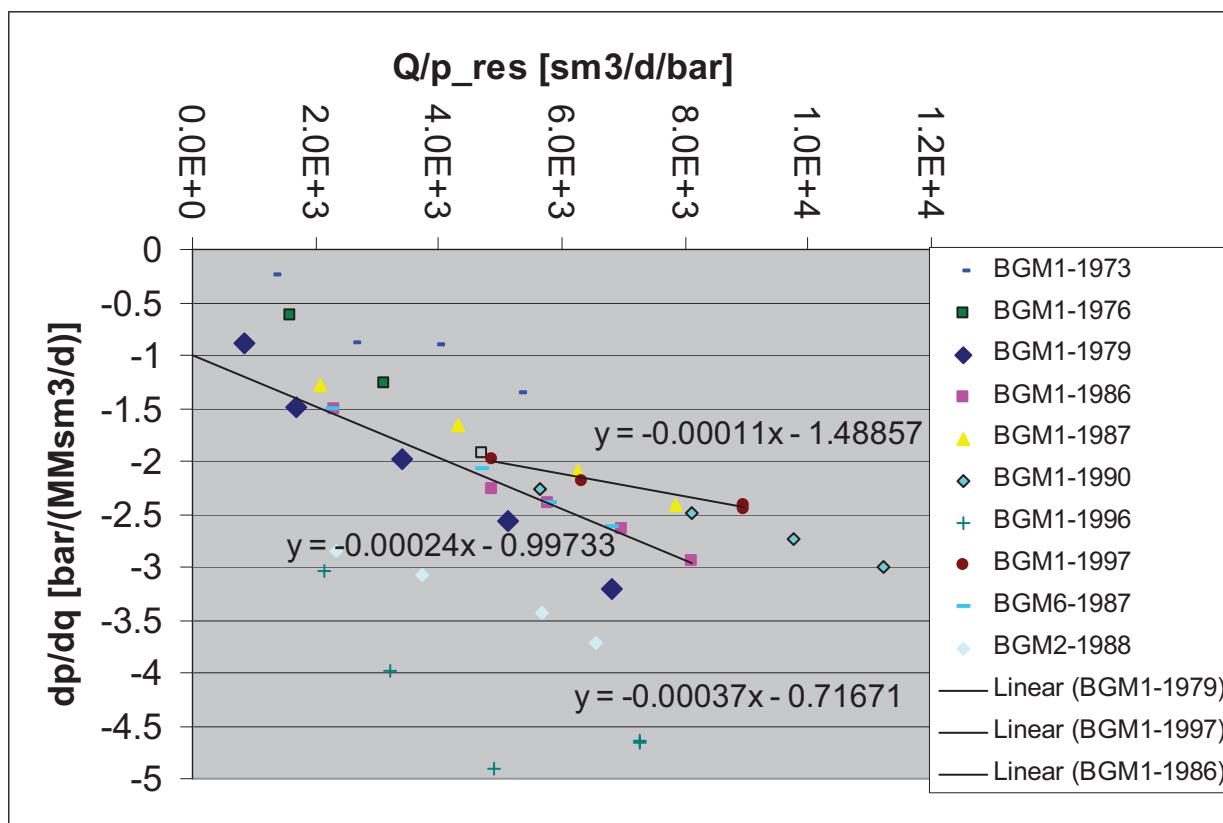


Figure 2-8 Plot showing rate-dependant pressure drop in historical well test data. The gradient is an indication of rate-dependant skin; the intercept indicates the mechanical skin value. The BGM-1 test (1979) was used as a reference for rate dependant skin, with a factor 2 higher and 4 lower as sensitivity.

2.5 History Matching Alternates

As discussed already in the phase 1 report [1], the well test build-up interpretation initially suggested lower permeabilities (Table 2-6, Table 2-5) than the history match. In the history match, it is mainly the GWC rise and the water production that limit the permeability downwards (and, clearly, in addition the historical rates need to be reached). The so-called 'DISMID_HIGHKV' model (section 2.3) was an adaptation of the model to cope with this, but succeeded only partially [1].

In order to have a pessimistic alternate subsurface model, some work was done to find the lowest permeability model that is allowed by the data. To the permeability model, there are two aspects:

- Average permeability in the gas zone
- Permeability contrast between the central and upper reservoir zone.

The former is the permeability corresponding to that seen in the well test. Lower permeabilities will lead to higher GWC's via what is in essence coning (Figure 2-12).

The latter has a double impact, as described in the phase 1 report [1]. Firstly it governs the permeability ratio between the BGM7-block (who sees the top reservoir zone only), and the MAIN block of BGM1 (who sees mainly the central reservoir zone). Secondly, at the fault area between the BGM7 and BGM-main

blocks, it governs the ratio between permeabilities in the gas zone and those in the water zone (Figure 2-9). If the contrast is high, the pressure equilibration between BGM7 and BGM-main will take place to a significant extent by BGM7→BGM-main water flux. If the contrast is low, the higher mobility of the gas will outweigh the lesser vertical height, and the gas flux will dominate. Thus, in the high-contrast case water flowing from BGM7→BGM-main will increase the GWC rise in BGM1.

The alternate models are generated from the 'DISMID_HIGHKV' model by application of an adhoc multiplier that is lower at the top and higher in the middle. In that way we can increase the BGM7/BGM1 permeability contrast, and modify the overall permeabilities. The reason for this is that the base DISMID_HIGHKV appears to underestimate the BGM7/BGM1 contrast (in addition to appearing somewhat too optimistic on overall levels), as indicated in Figure 2-10. Values are shown Table 2-7. Figure 2-11 shows an example of the multiplier and of the result on the permeability in the gaszone . The BELL profiles still give somewhat higher permeabilities at the BGM7 location than estimated from well tests. Hence the LOG_BELL realization was added.

It should be noted that the overall per-field multipliers are applied on top. Thus GRT remains with lower permeability multiplier as in the phase 1 report [1] (this can be seen in the north of Figure 2-11, right plot). If we history match these realizations, we see that they do not all work. If we take the BELL realizations below 033, the water production (and contact rise) is excessive. Similarly, the LOG_BELL realizations do not work at all (Figure 2-15).

The BELL_033 run, on the other hand, does have a mismatch on both water and GWC (Figure 2-15), but they are modest. Figure 2-13 shows the pressure match, which also is modest. To achieve this, the BELL_033 run has a substantially higher fault seal factor at the inferred fault between the two BGM blocks (Table 2-7). Therefore this is a reasonable pessimistic case. The conclusion is therefore still that well test and history match permeabilities still show some discrepancy.

Realization	BGM Multiplier (top/center)	MULTFLT for 2B alt2
DISMID_HIGHKV	1/1	0.0005
DISMID_HIGHKV_BELL_100	0.5/2	0.0008
DISMID_HIGHKV_BELL_050	0.25/1	0.050
DISMID_HIGHKV_BELL_033	0.17/0.67	0.025
DISMID_HIGHKV_BELL_025	0.13/0.5	1.0 [i.e. fully open]
DISMID_HIGHKV_LOG_BELL_100	0.03/1	1.0 [i.e. fully open]

Table 2-7 Multiplier values of 'BELL' realizations to create a pessimistic subsurface case. In the 'BELL' realizations, the multiplier has a parabolic profile, in the 'LOG_BELL' realizations the logarithm of the profile is parabolic

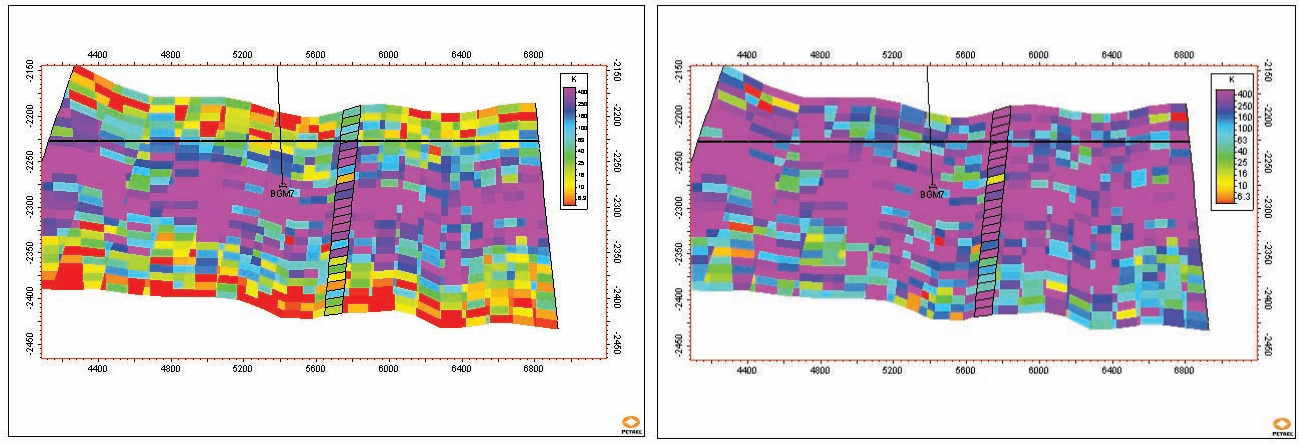


Figure 2-9 Roughly SW/NE cross-section through BGM7 (plotted in black). The inferred fault between the BGM7 and BGM-main blocks is also shown (stack of outlined blocks), as is the original GWC. The property plotted is permeability (5-500 mD). The left plot shows a high contrast model (DISMID_HIGHKV_LOG_BELL_100), the right plot a low contrast model (DISMID_HIGHKV).

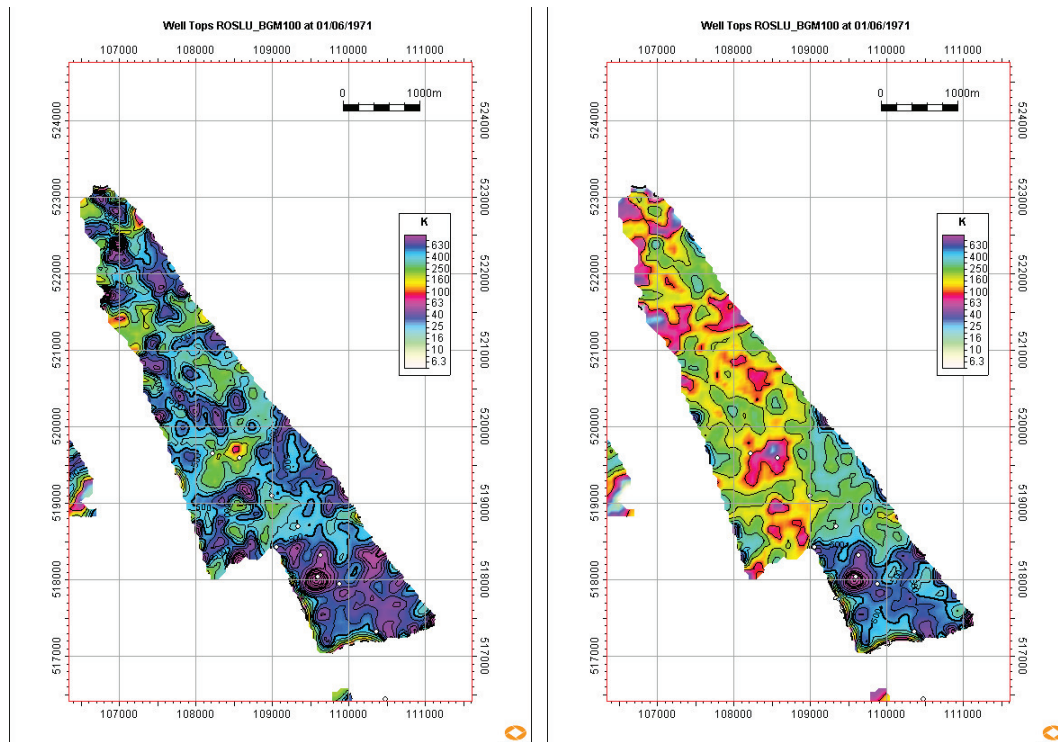


Figure 2-10 Average permeability maps over the gas zone. Left is the 'DISMID_HIGHKV' model (High Case), average permeability values at BGM7/BGM1 are roughly 300/800 mD. Right shows the 'DISMID_HIGHKV_BELL_050' model (Mid Case), average permeability values at BGM7/BGM1 125/750 mD. The 'BELL_033' run (Low Case) has 2/3 of the 'BELL_050' run (i.e. 85/500 mD).

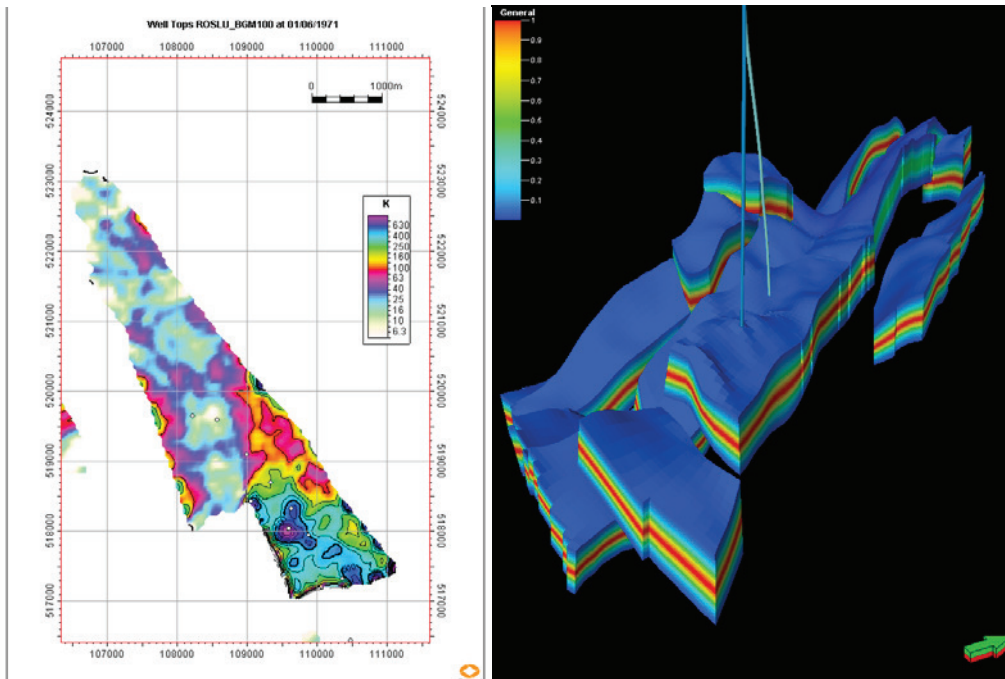


Figure 2-11 Gas zone average permeability map of the 'DISMID_HIGHKV_LOG_BELL_100' realisation on the left (unmatchable). BGM7/BGM1 have permeabilities of ca 20/600 mD. Permeability multiplier used for the 'LOG_BELL_100' case (1 in the middle and 0.03 top/bottom). The wells BGM1 (dark blue) and BGM7 (light blue) are plotted for reference.

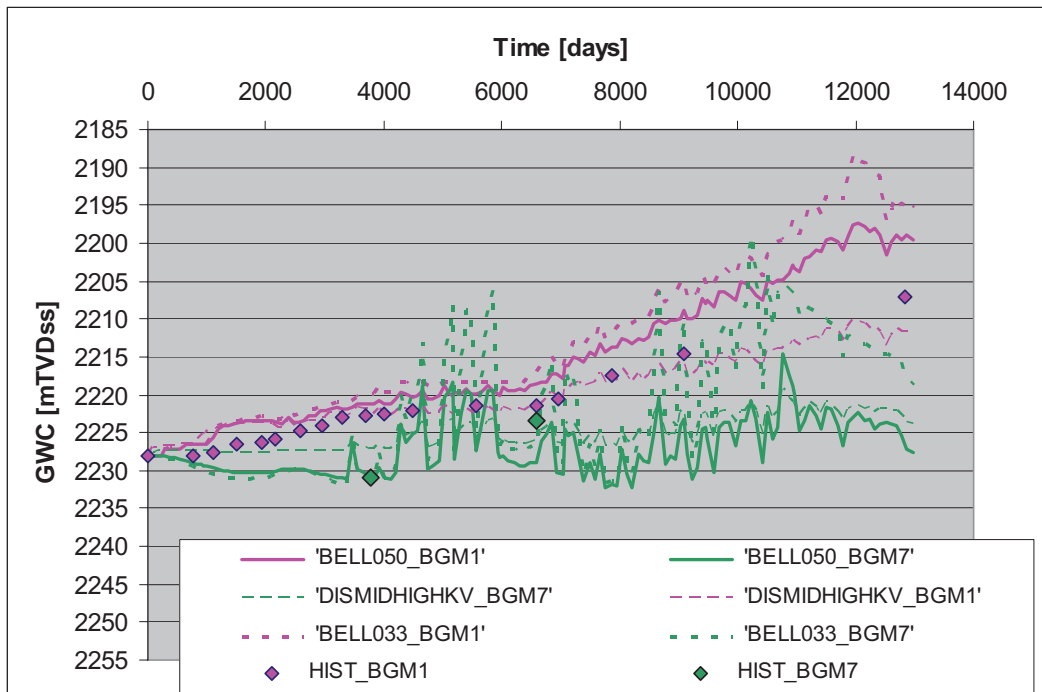


Figure 2-12 GWC behaviour of BELL_033 (low case) and BELL_050 (mid case) sensitivities. In BGM1, the GWC is 2207 m tvdss at the end of history; BELL_050 and BELL_033 have a GWC of 7, resp. 13 m too shallow due to coning. In BGM-7, the BELL_050 and BELL_033 fit very well at the start, but BELL_033 is much too shallow at the end.

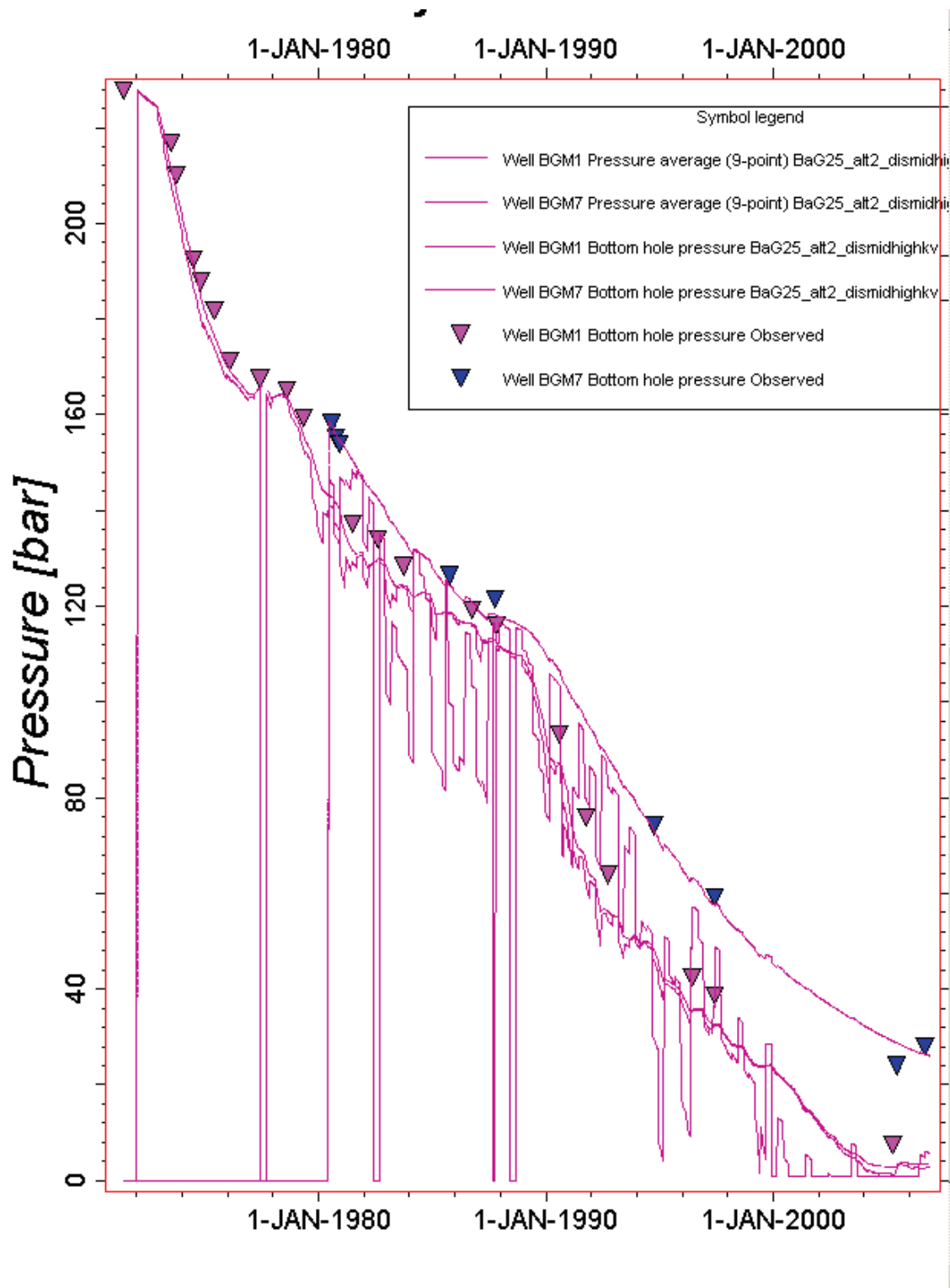


Figure 2-13 Pressure match for the BELL_033 alternate. Pressures plotted are the BHP's and the gridblock pressures (9-block average, "WBP9"). For BGM7 the BHP goes to zero, indicating that the historic rates cannot be matched anymore after 2007. Pressures in the main block are somewhat too low, but increasing the fault seal would lower BGM7 pressures (which would make it fail even earlier).

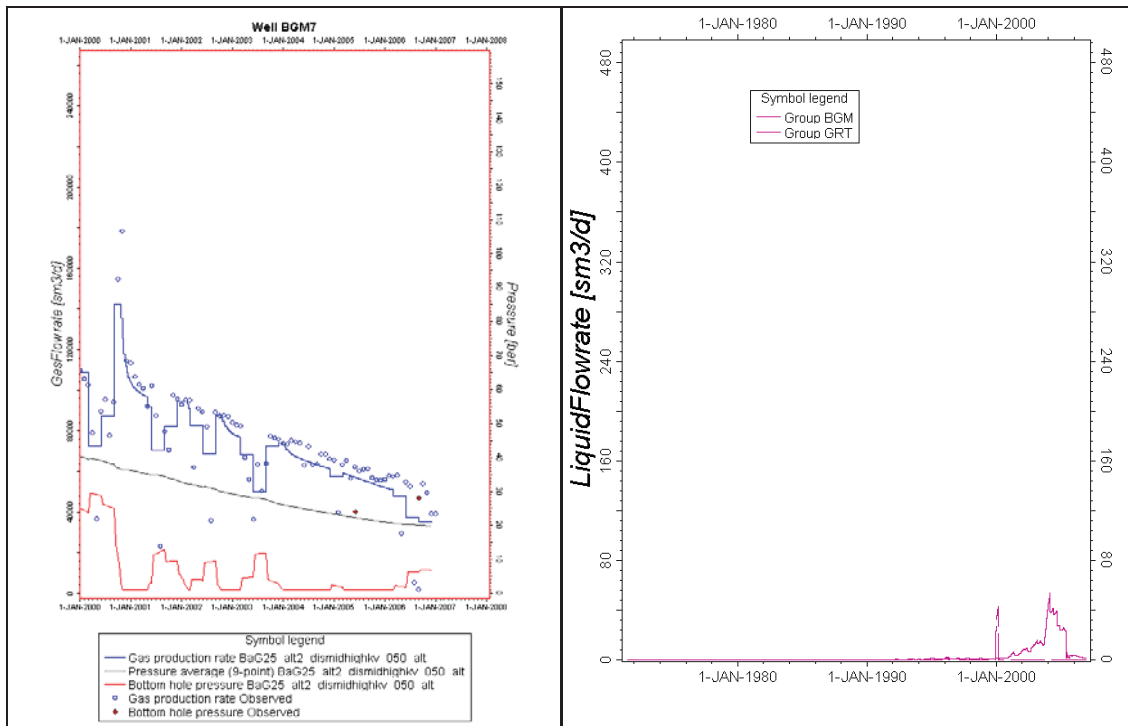


Figure 2-14 Left: Late BGM7 history (pressue & rates) showing rates are not met due to BHP limit [BELL_033]. Right: Water production rates for BELL_033.

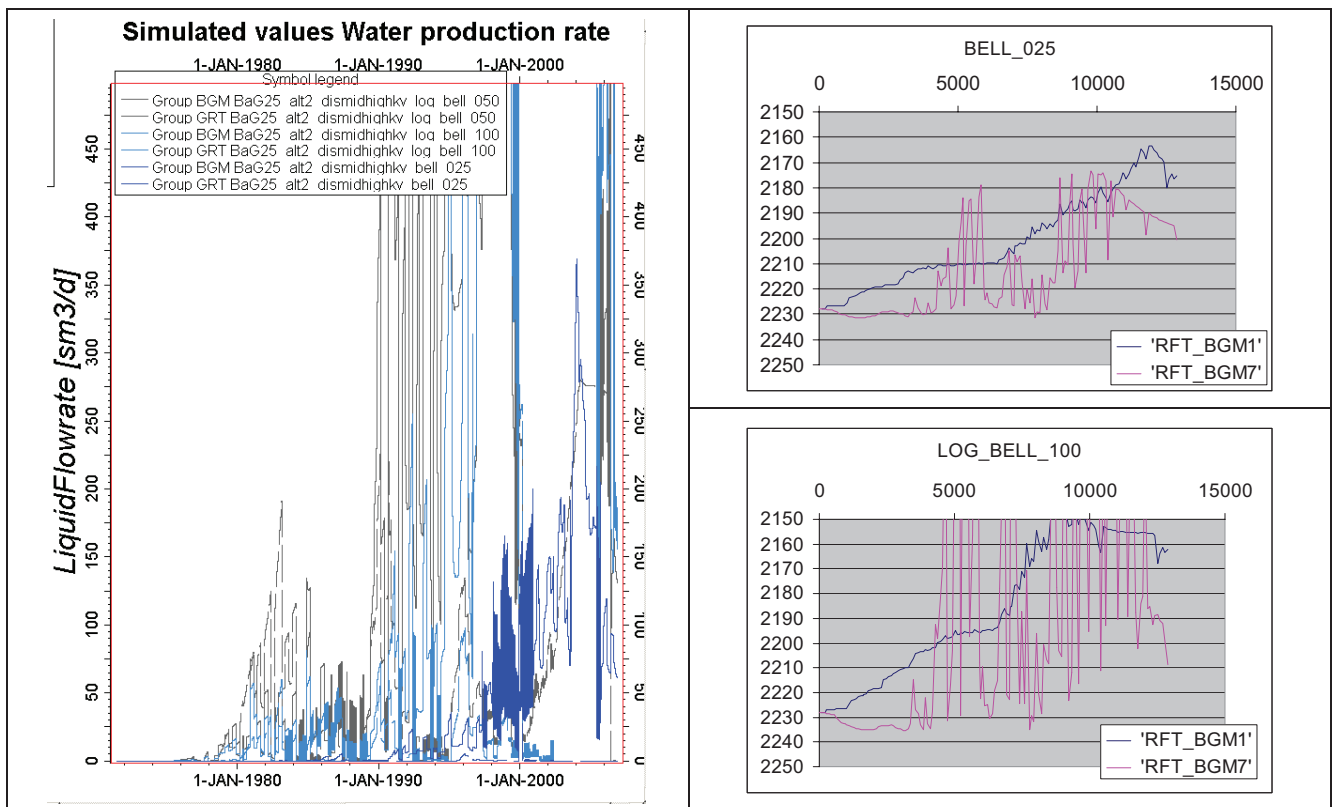


Figure 2-15 Water production (left) and GWC rise (right) for too-pessimistic runs ('BELL_025' and 'LOG_BELL_100'). Historical GWC data give values of about 2207 m at the end of the historic period. It should be noted that the GWC's extracted for BGM7 in the 'LOG_BELL_100' case are somewhat distorted due to the water production.

3 Well Performance Modelling

The present phase, focusing more on the UGS performance, required more extensive & detailed wellbore modelling, as well as good handling of inflow performance. Use was made of well modelling software Prosper, version 10.0, or IPM version 6.0.

3.1 Inflow performance model BGM-1

The inflow performance of BGM-1 (1979 test data) was revisited in order to better calibrate non-Darcy effects around the wellbore in the simulation model. The other main objective was to look at the relative importance of skin in the reservoir vs. skin in the tubing at the high rates to be used in the UGS phase. In prosper this was done using the Multi-Rate Jones model. Advantages of this inflow model over the Forchheimer model used in the previous phase, is that the model will calculate the reservoir pressure automatically from the test-data points. Also, the model better reflects low-rate flow-behaviour. For reservoir parameters and the downhole equipment data is referred to the previous report [1], Table 6-1 and Table 6-3. PVT tables as used for the dynamic model were directly imported to Prosper to avoid a PVT-correlation mismatch. The Jones equation can be expressed in the form

$$P_R^2 - P_{wf}^2 = AQ + FQ^2,$$

where P_r is the reservoir pressure, P_{wf} is the bottom hole flowing pressure, A is the Darcy flow-coefficient for laminar flow and F is the non-Darcy flow coefficient for turbulent flow around the wellbore. The values for A , F and Absolute Open Flow potential (AOF) as found by matching the isochronal test-data are

$$A = 2.6 \text{ E-4 } \text{bar}^2/(\text{sm}^3/\text{day}),$$

$$F = 7.0 \text{ E-10 } \{ \text{bar}^2/(\text{sm}^3/\text{day}) \}^2,$$

$$\text{AOF} = 5.73\text{E6 } \text{sm}^3/\text{day}.$$

The values differ from the values found with the Forchheimer model in the previous phase. These were AOF 3.93E6, A 3.0E-4 and F 1.5E-9. The difference was very likely caused by the internal Prosper PVT correlation that resulted in a Z-factor that was previously 10% too low for the gas. The inflow performance plot of the 1979 well test in BGM-1, as described by the above parameters, is shown in Figure 3-1.



Figure 3-1 IPR plot BGM-1 using isochronal test results of 1979.

3.2 VLP / IPR matching BGM-1

After the inflow performance of the multi-rate test was matched, the vertical lift performance was also checked with BHP and THP values from the test. This VLP-matching was done with the Gray-correlation, which is thought to be most suitable for gas wells. Results are shown in Figure 3-2. It can be seen that the MultiRate Jones model has improved the match when compared to matching done in the previous phase with the Forchheimer inflow equation, see Figure 6-3 and Table 6-6 [1]. Two other conclusions were drawn from the IPR/VLP matching exercise:

- the 7% gravity term correction in the Gray-correlation could be adjusted by increasing the CGR from 0 to 0.5 stb/MMscf (2.8 l./Mm³ gas),
- the 40% friction term correction was very sensitive to the roughness of the tubing.

Without the CGR correction in the PVT, the gravity term correction calculated by the Gray correlation was 1.07. The friction term correction was 1.40 which means that the measured friction pressure loss was much bigger than that calculated with the Prosper input parameters. The main influence on the friction term was the inside tubing roughness. Initially this was set to 0.0005" (0.00127 cm), but with a 10 times rougher tubing, the friction term became smaller than 1. The friction term multipliers for varying tubing roughness are given below:

- 5e-3" → multiplier friction term 0.94

- 5e-4" → multiplier friction term 1.40
- 5e-5" → multiplier friction term 1.89

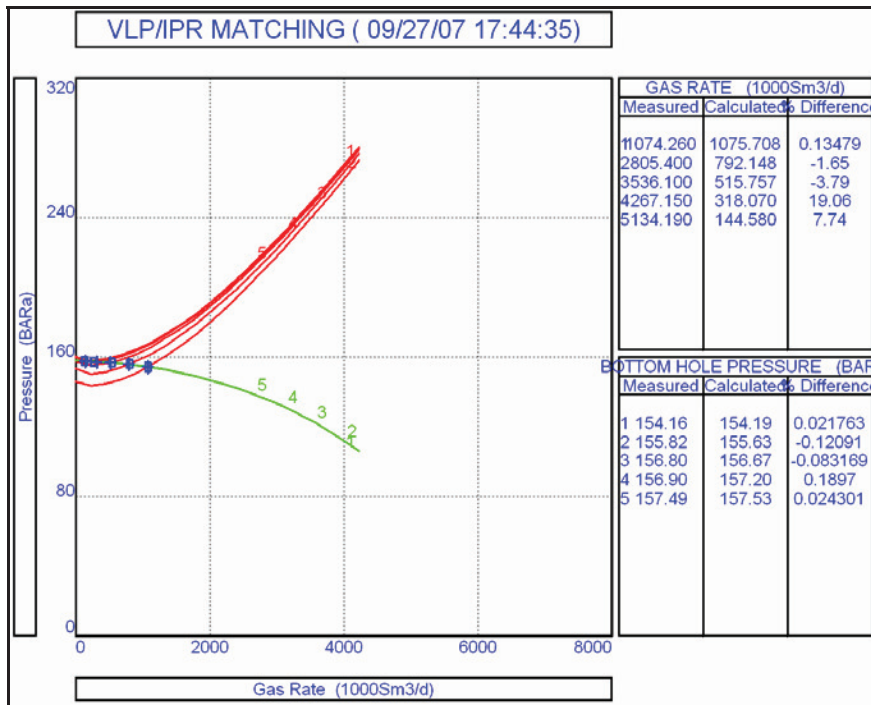


Figure 3-2 VLP/IPR matching results BGM-1 multirate test-data (1979), MultiRate Jones IPR model and matched VLP parameters

The roughness results were of importance for creation of the lift curves in the forward model. Sensitivity results for skin, permeability, WGR, CGR, tubing roughness and tubing diameter are presented in section 3.6. The lift performance curves for the development wells are given in section 3.4.

3.3 Description of non-Darcy skin in Eclipse

In the Eclipse model, the non-Darcy pressure drop is implemented via the flow dependent skin factor D. The D-factor was specified in the previous phase by the keyword WDFAC in Eclipse, and was found by matching the BGM-1 inflow performance seen during the 1979 well-test. Using WDFAC for the development wells was however not found suitable as the new wells would also be drilled in much worse quality reservoir than around BGM-1. Also, the total horizontal well-length of 500m is much greater than the originally perforated length in BGM-1 of 17m. Therefore the keyword WDFAC was replaced by WDFACCOR, which uses a correlation that incorporates porosity, permeability, well-radius and length. Because WDFACCOR is calculated for each connection in the well, the total well-skin becomes

$$S_w = S + \sum_j D_j q_j$$

where q is the free gas-flow rate at each well-connection. An expression for the D-factor as found by Dake [2] is given by

$$D = \alpha * \beta * \frac{k}{h} * \frac{1}{r_w} * \frac{\gamma_g}{\mu_g},$$

where

α is the viscous flow conversion factor calculated for certain pressure, temperature and air density values at standard conditions

β is the coefficient of inertial resistance for non-Darcy flow [1/m]

k is the permeability of the connected gridblock [mD]

h is the length of the connection [m]

r_w is the wellbore radius [m]

γ_g is the relative gas-density to air at s.c. [g/cc]

μ_g is the gas viscosity at bottom hole pressure [cP]

From laboratory experiments Dake finds a value of $\alpha = 2.223 \times 10^{-15}$ in field units as conversion factor (2.228×10^{-18} in metric units). A relationship between the coefficient of inertial resistance β and the absolute permeability was determined in the laboratory by experiments on sandstone plugs according to

$$\beta = const. * k^B * \phi^C.$$

Values found by Dake are $const. = 2.73 \times 10^{10}$, $B = -1.1045$ and $C = 0$ in field units or $const. = 8.32 \times 10^{11}$, $B = -1.1045$ and $C = 0$ in metric units. β in Dake has dimensions of [1/ft] in field units and [1/cm] in metric units. Rewriting the formula for the D-factor with $\beta = k^B * \phi^C$ and $\alpha = \frac{A}{const.}$, it can be rewritten for the use of A, B and C

values in the WDFACCOR keyword in Eclipse:

$$D = A * k^B * \phi^C * \frac{k}{h} * \frac{1}{r_w} * \frac{\gamma_g}{\mu_g}.$$

The standard values for A, B and C as described by Dake in field units are $A = 6.068 \times 10^{-5}$, $B = -1.1045$ and $C = 0$, or $A = 1.85 \times 10^{-6}$, $B = -1.1045$ and $C = 0$ in metric units. The A-coefficient was checked against well test data from Bergermeer-1 (1979), to reflect the Bergermeer reservoir rather than the laboratory

measurements in Dake. This resulted in the final values for WDFACCOR as put into Eclipse:

A=1.6e-6, B=-1.1045, C=0.

Figure 3-3 shows the match of the WDFACCOR keyword with the previously used value for WDFAC. The well-test of BGM-1 shows the non-Darcy pressure drop in the FBHP values at different gas-flow-rates. For the initial matching of WDFAC is referred to section 6.1.5 of the phase 1 report, Ref [1].

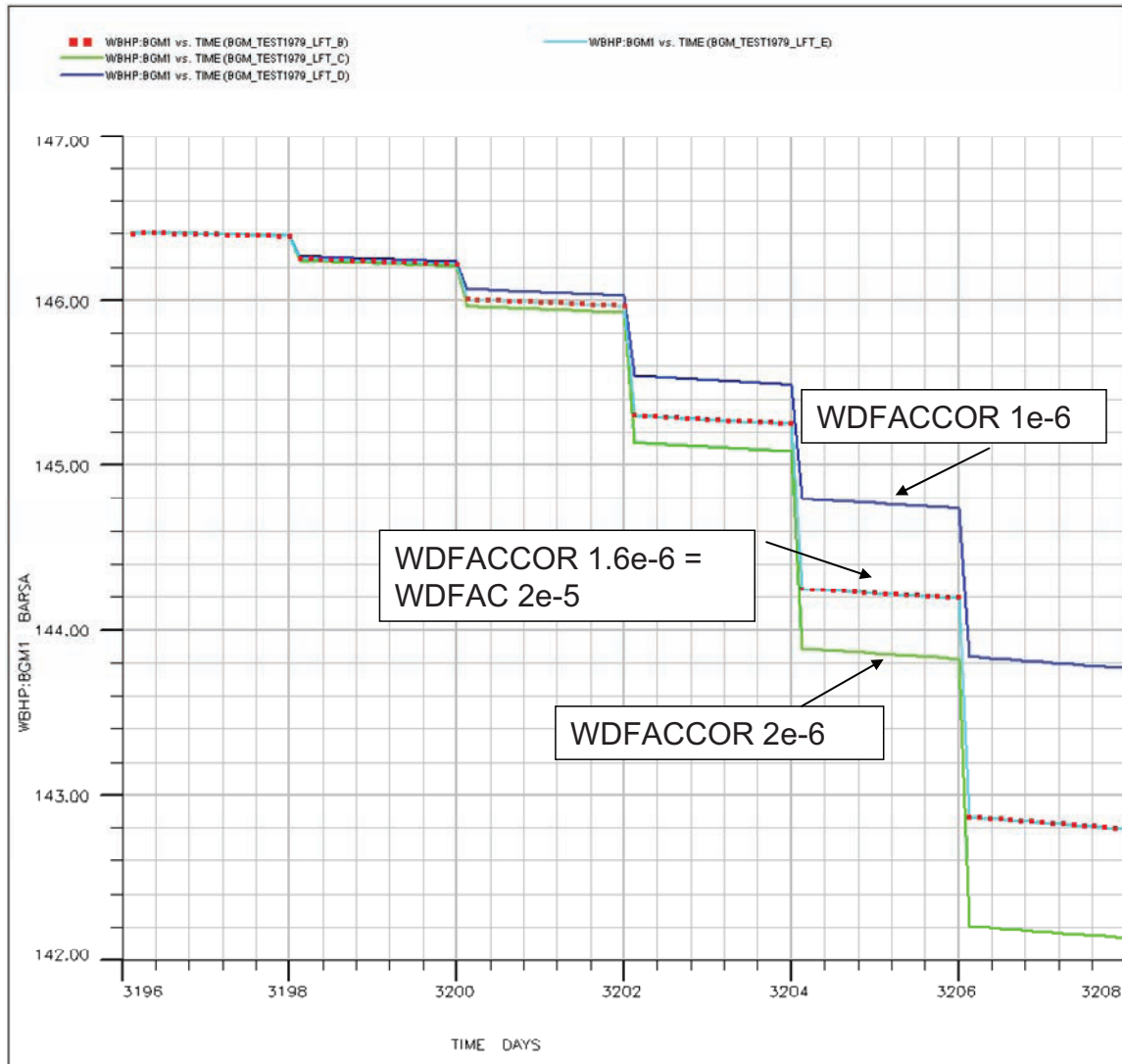


Figure 3-3 WDFACCOR match in Eclipse to multi-rate test BGM-1 (1979). The light blue line (WDFACCOR = 1.6e-6) overlays the green line of the previous HM (WDFAC = 2e-5).

3.4 Lift curves

In the Eclipse model, the lift performance was captured as lift tables, exported from the various Prosper cases. Prosper version 10.0 / IPM version 6.0 were used. The UGS wells were divided into two broad categories: horizontal and vertical. Differences within the categories were neglected. Separate tables for production and injection were generated. The input parameters for the vertical and horizontal wells are

given in Table 3-1.

	Vertical well	Horizontal well
Tubing length [m]	2200	3600
Tubing size [inch]	7 5/8"	7 5/8"
Roughness [m]	3.175e-6	3.175e-6
CGR [l./Mm3]	2.8	2.8

Table 3-1 Main lift curve input parameters for vertical and horizontal development wells

The 2200 m tubing length of the vertical well is the expected MD at top reservoir (ca 2000 m tvdss). The horizontal tubing length of the future development wells is expected to average at ca 3300 m, but 3600 m was taken in order to be on the conservative side. The CGR was increased in the VLP/IPR matching exercise from 0 to 0.5 stb/MMscf in order to reduce the gravity term multiplier in the Gray correlation from 1.07 to 1.00. The roughness was changed from 0.0005" (0.00127 cm) for normal steel quality to 0.00015" (0.00032 cm) for stainless steel tubing.

Figure 3-4 shows VLP / IPR curves plotted. The IPR is described by the multirate-Jones model and was obtained by matching well test data of BGM-1 from 1979 (see section 3.2). The VLP input parameters are given in Table 3-1. Parameter sensitivities are run later in this section. Figure 3-5 shows the VLP / IPR curves for a horizontal development well. The horizontal IPR model used was by Kuchuk & Goode, which did not include any flow-boundaries. The main input parameters are given in Table 3-2.

Horizontal length	500	m
Permeability	50	mD
Res. height	100	m
OH radius	4.5	inch
Kv/Kh	0.1	
WGR	0	stb/MMscf
CGR	0.5	stb/MMscf
Skin	0	
D	1.80E-08	1/(Sm3/d)

Table 3-2 IPR model parameters for horizontal well in Prosper

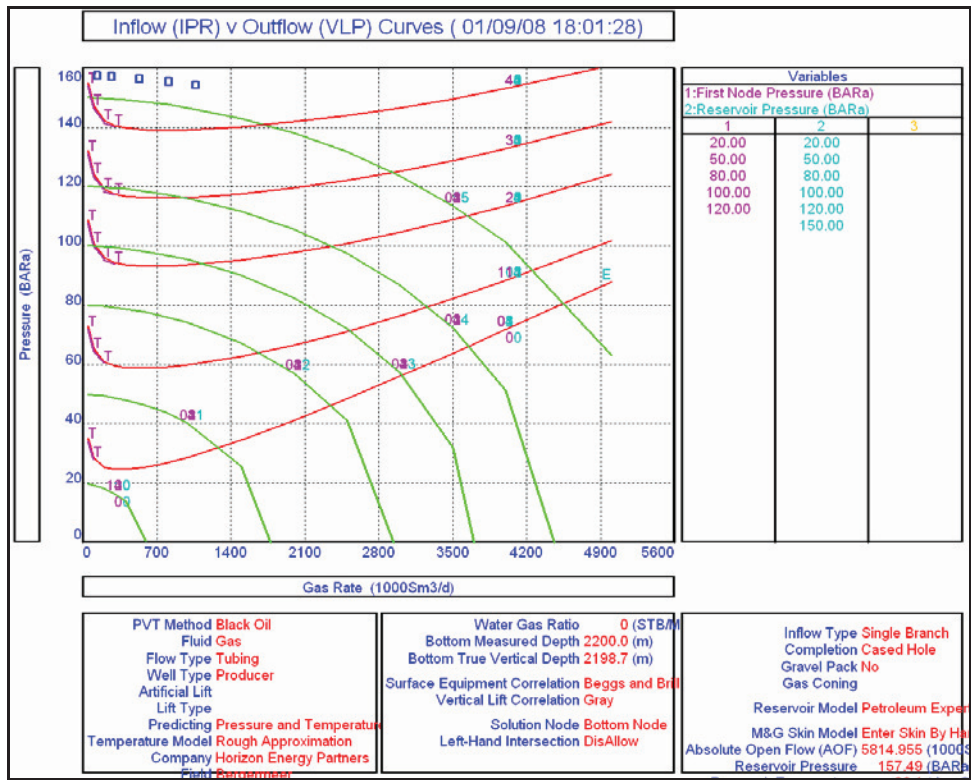


Figure 3-4 IPR / VLP plot for vertical well model, IPR from well test match BGM-1

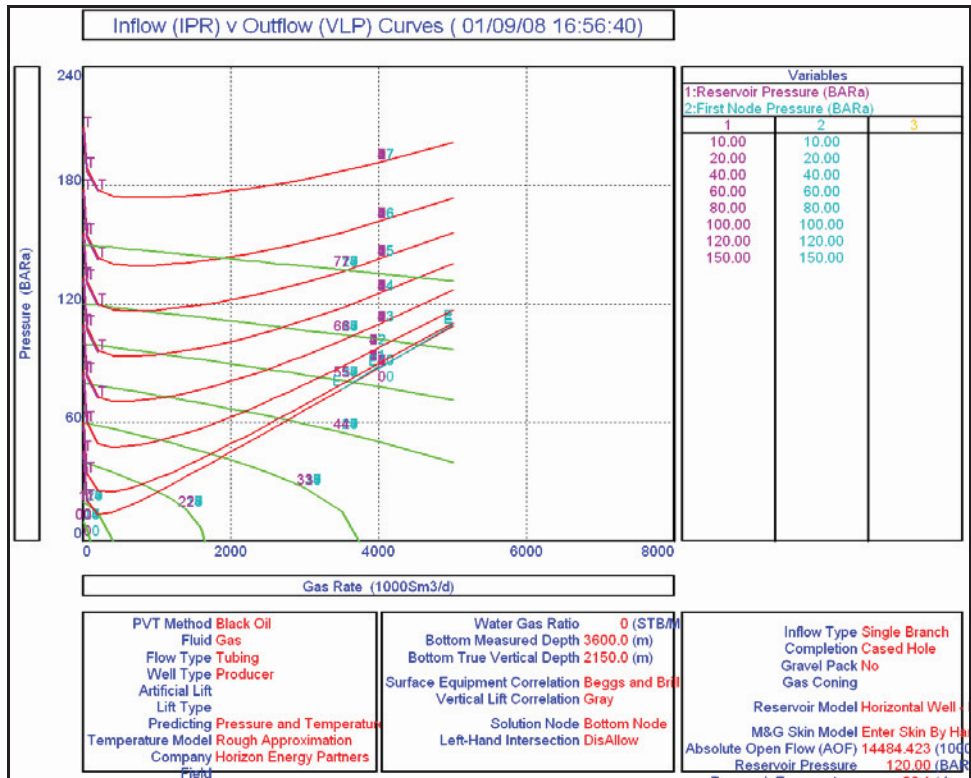


Figure 3-5 IPR / VLP plot for horizontal well model, IPR model Kuchuk & Goode

3.5 Friction versus gravity losses in tubing (Pressure vs Depth)

Pressure-versus-depth plots were constructed in order to check the relative contributions of friction vs gravity losses in the horizontal tubing. These are given for the horizontal well model, P_reservoir 120 bar, FTHP 80, resp. 40 bar, in Figure 3-6 and Figure 3-7. It can be seen that at 2.7 MMm3/d, the pressure drop in the tubing (28 bar) is already greater than around the well (12 bar). Most of this pressure drop in the tubing (60%) is due to friction losses. At 4.1 MMm3/d, the pressure loss in the tubing of 60 bar is much more than around the well (19 bar). Now 85% of pressure drop in the tubing is from friction losses.

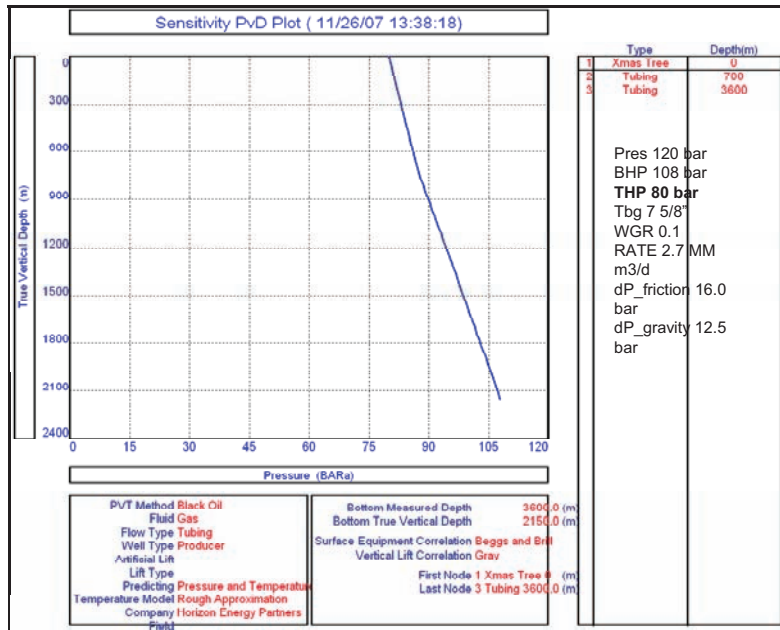


Figure 3-6 Pressure vs Depth horizontal well model, Pres 120 bar, THP 80 bar

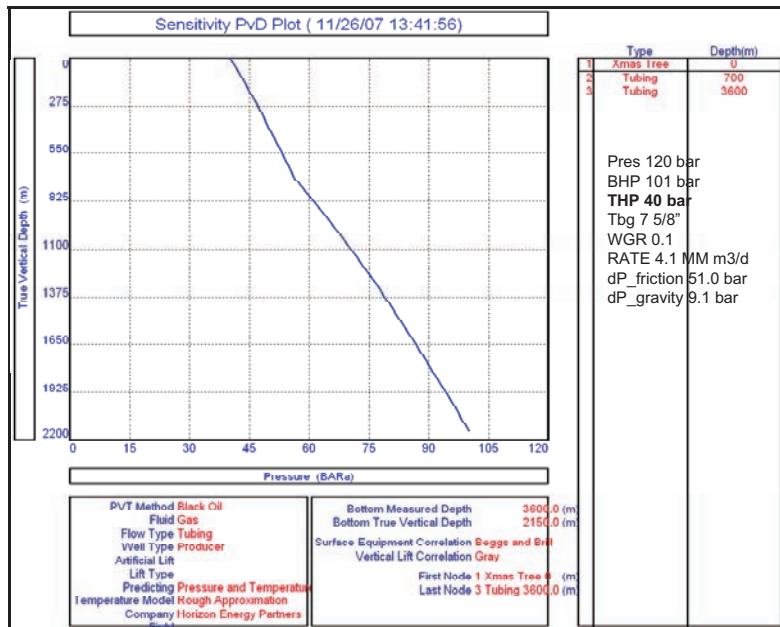


Figure 3-7 Pressure vs Depth horizontal well model, Pres 120 bar, THP 40 bar

3.6 IPR / VLP sensitivities

Sensitivities were run on tubing size, roughness, skin, permeability, water-gas-ratio and condensate-gas-ratio. The values used to generate a Prosper base case are given in the table below. In hindsight, the base case permeability value for vertical inflow performance is closer to ca 600 mD instead of 200 mD.

Sensitivity	Permeability [mD]		Skin	CGR [m3/m3]	WGR [m3/m3]	Tbg. Roughness	Tubing-size OD
Prosper	Vert. Well model	Hor.well model		(stb/MMscf)	(stb/MMscf)	[inch]	[inch]
Base Case	200	50	0	3 (0.5)	0	0.00015	7 5/8"

Table 3-3 Base case values used for well performance sensitivity calculations.

3.6.1 Skin

The Prosper inflow models as discussed in the previous paragraph were used to see the effect of skin on well performance. Historically, the skin values found in Bergermeer varied between ca -3 and 10, see Table 5-8 of the previous report [1]. The base case forecasts have skin=0. For the vertical well model, the effect is shown in Figure 3-8. The permeability is 200 mD. For a reservoir pressure of 120 bar, and a WHP of 80 bar the gas-rate varies only between 2.2 and 2.3 MMsm3/d.

The horizontal well has more exposure to the reservoir and is therefore more influenced by higher skin-values. Figure 3-9 shows the effect of Skin on the horizontal well model in Prosper. The permeability is 50 mD. At a reservoir pressure of 120 bar and a WHP of 80 bar, the gas-rate is shown to vary between 2.1 and 2.7 MMsm3/d.

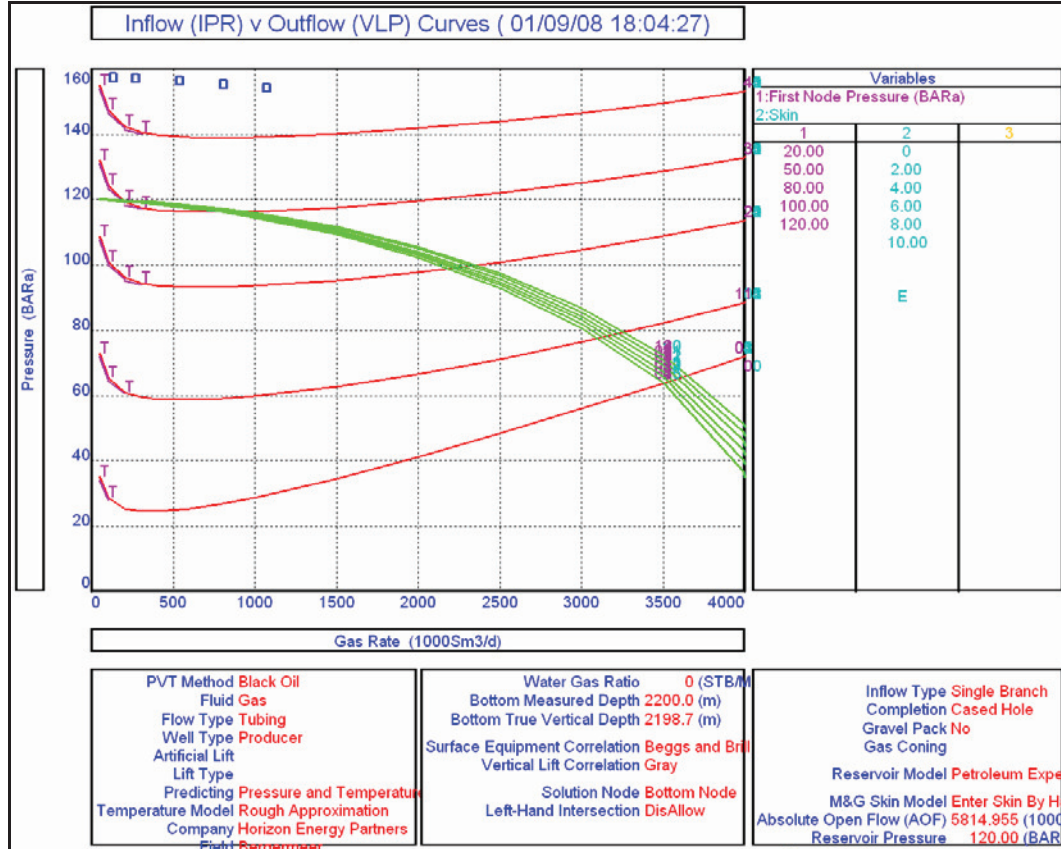


Figure 3-8 Effect of Skin on IPR of vertical well.

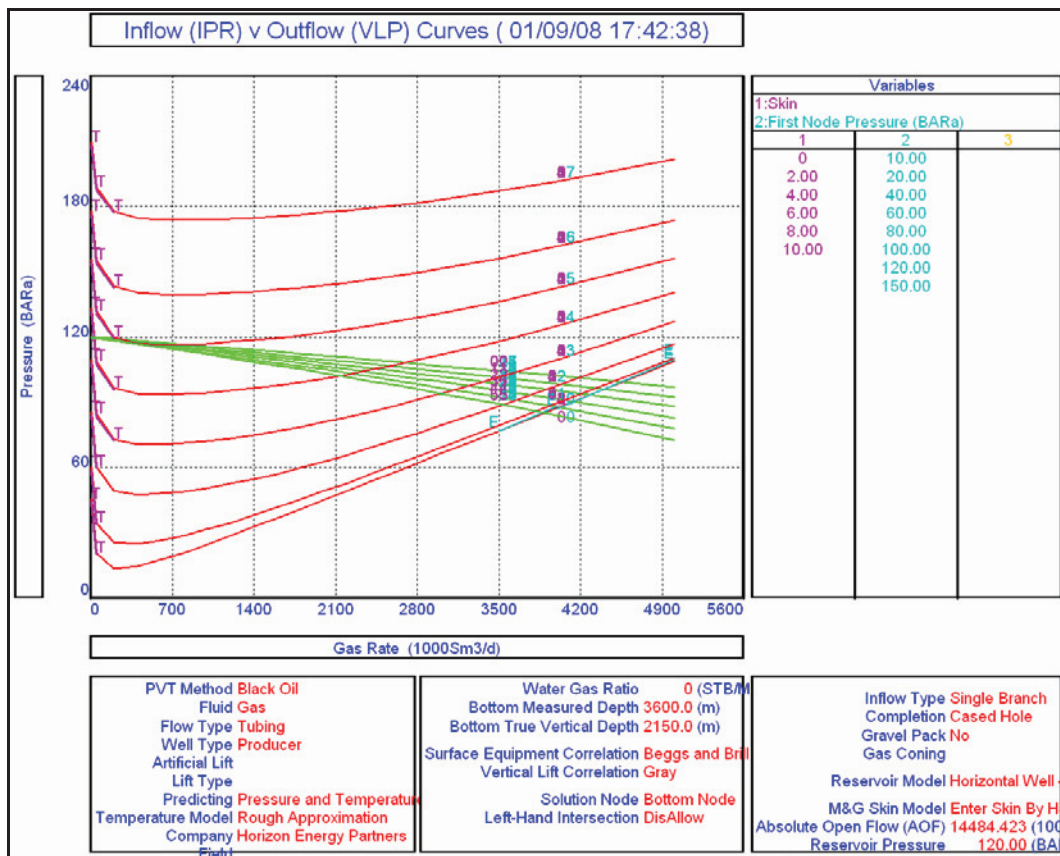


Figure 3-9 Effect of Skin on IPR horizontal well

3.6.2 Permeability

The effect of permeability changes on the IPR model is significant. Figure 3-10 gives the effect on the vertical well model. Between 100 and 1000 mD, a reservoir pressure of 120 bar and a WHP of 80 bar, the same tubing will produce between 1.7 and 3.7 MMsm3/d. For a horizontal well, a permeability difference between 10 and 100 mD, P_{res} 120 bar, WHP 80 bar, results in gasrates of 1.1 resp 3.1 MMsm3/d. It is therefore important to know what permeability can be expected in the reservoir at the locations of the new wells. The permeability is the main geological parameter and was therefore varied for the different forecast cases, see section 5.2.

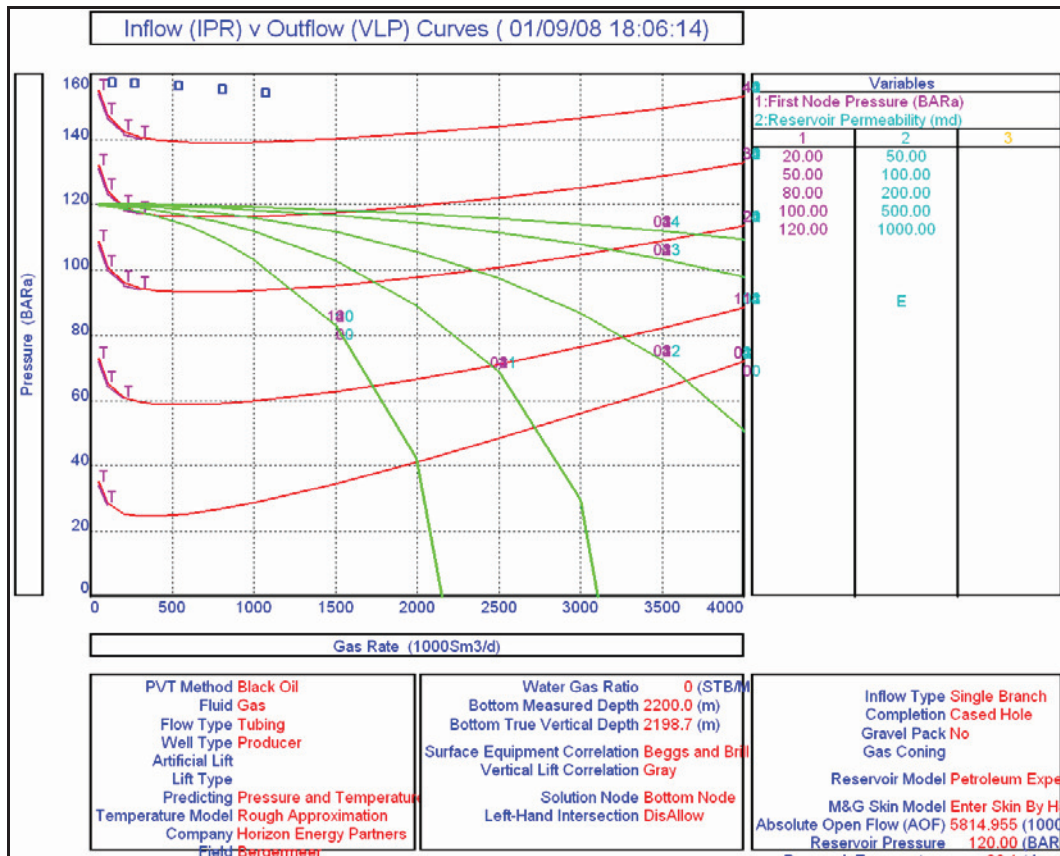


Figure 3-10 Permeability variations on vertical well IPR model

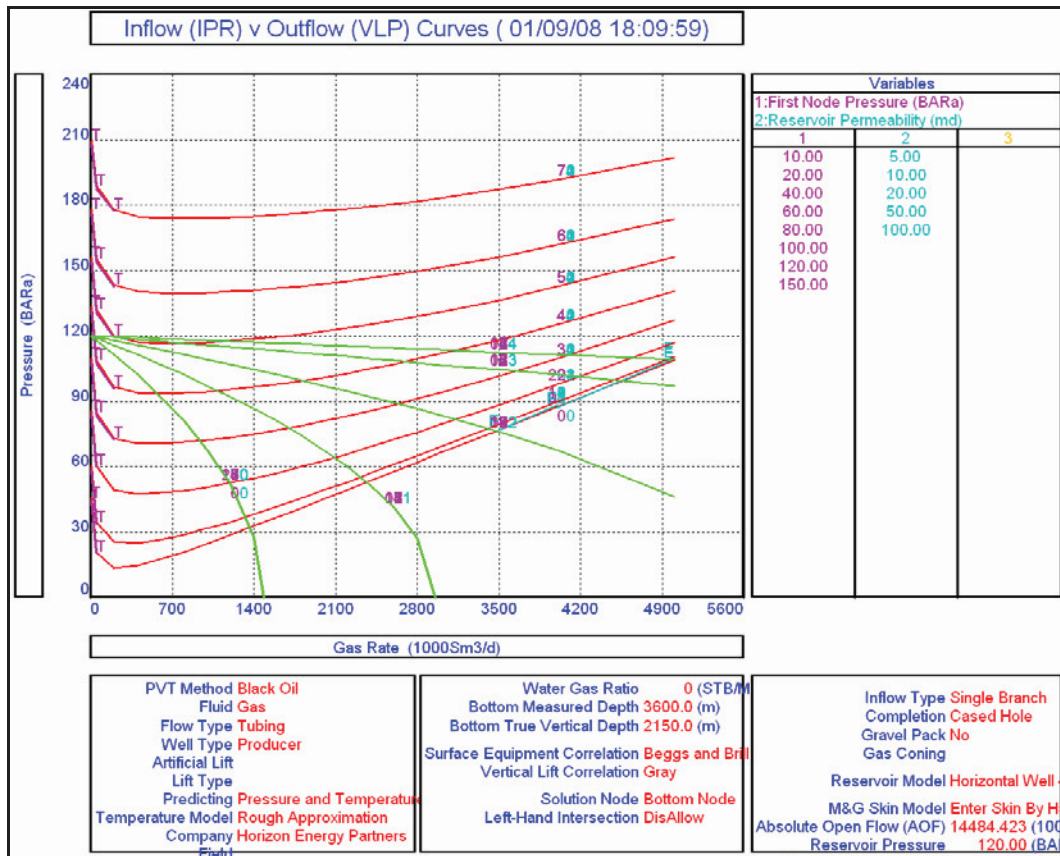


Figure 3-11 Permeability variations on horizontal well IPR model

3.6.3 CGR

Historically, the condensate-gas-ratios values produced from Bergermeer were low (but figures from the early history are absent, and PVT data on CGR is missing). Production data from BGM-1 shows values between 14 and 6e-6 m³/m³ (1 stb/MMscf), see Figure 5-3 in [1]. There was not sufficient data to include condensate in the PVT-model. The lift curves were however constructed with a CGR of 3e-6 m³/m³ (0.5 stb/MMscf) because this matched to the gravity component multiplier of well-testdata from BGM-1 (see section 3.2). In Figure 3-13 and Figure 3-13 the CGR-curves are plotted with WHP on the x-axis and gas-rate on the y-axis. Even at higher drawdowns, the effect of an increase in CGR from 0 to 56 m³/m³ (10 stb/MMscf) is minimal (less than 5%), see curve 4. CGR values in Bergermeer are within this range.

In line with an expected decrease in CGR during production, the CGR is expected to increase with the higher pressures forecasted for the UGS phase as the condensate that dropped out during production re-vaporizes during injection of undersaturated dry gas. In this respect it would be possible to look for CGR-information in Bergermeer test-data etc. at reservoir pressures that are expected during the UGS phase.

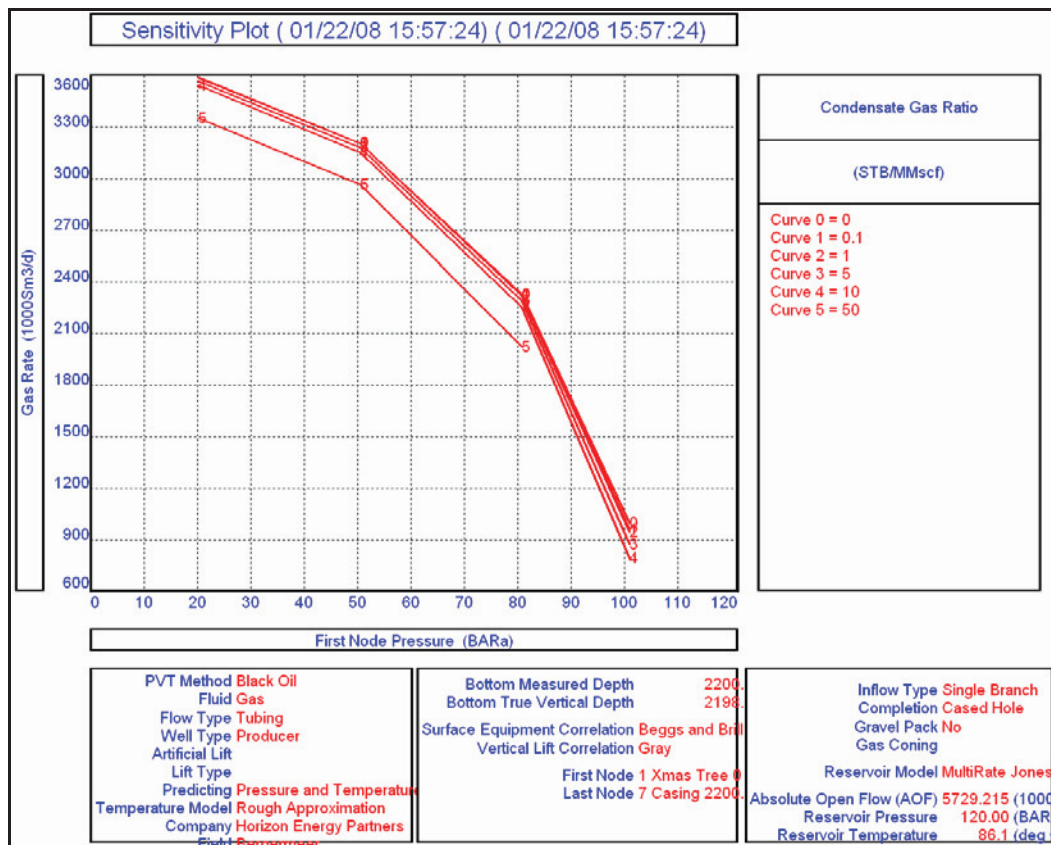


Figure 3-12 CGR sensitivity for vertical wells. The reservoir pressure is 157.5 bar.

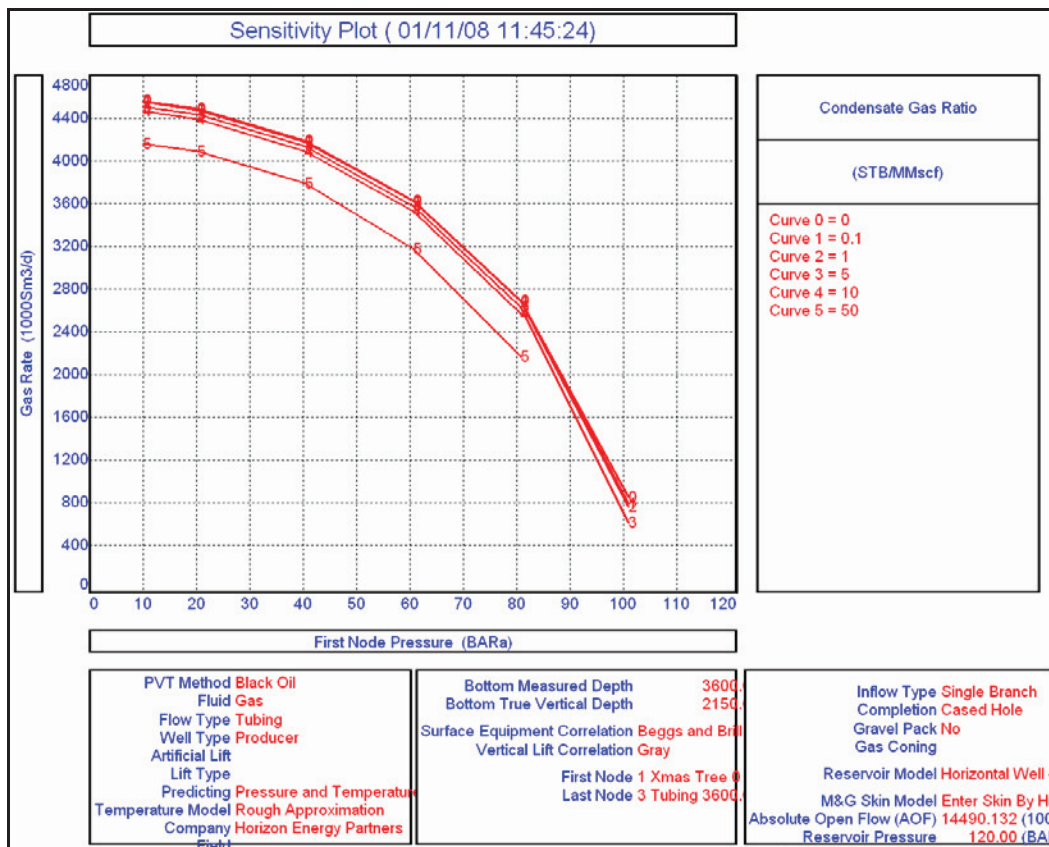


Figure 3-13 CGR sensitivity for horizontal wells. The reservoir pressure is 120 bar.

3.6.4 WGR

Taqa has mentioned a recent WGR as high as 17×10^{-6} m³/m³. This is due to water vapor, as no free water is produced (the free water is salt-saturated, so is easily distinguished from condensate water).

The WGR in the dynamic model is 0, since inclusion of water vapour would make the Eclipse PVT model complex, and the impact on the *subsurface* flow is negligible.

Running sensitivities in Prosper, we can see that the effect of an increase in WGR from 0 to 56×10^{-6} m³/m³ (10 stb/MMscf) on the *lift* performance is not negligible. For the vertical well model (see Figure 3-15) this results in an decrease in gas-rate from ca 4.0 to 3.7 MMsm³/d at Pres. 157.5 bar and WHP 80 bar. For the horizontal well model the decrease at Pres 120 bar and WHP 80 bar is from ca 2.7 to 2.0 MMsm³/d.

Apart from the possible water production by coning, the amount of condensed water that can be expected during the UGS phase can be deduced from its phase behaviour. Assuming that the reservoir temperature will not change, and assuming that the gas behaves as an ideal gas, the vapour pressure is more or less constant during the UGS phase. With an increase in reservoir pressure from ca 10 to ca 100 bar or a factor 10, the amount of water-vapour in the gas will be reduced by a factor 10. The risk of water-coning is discussed in section 5.4.2 on GWC movement in the UGS phase.

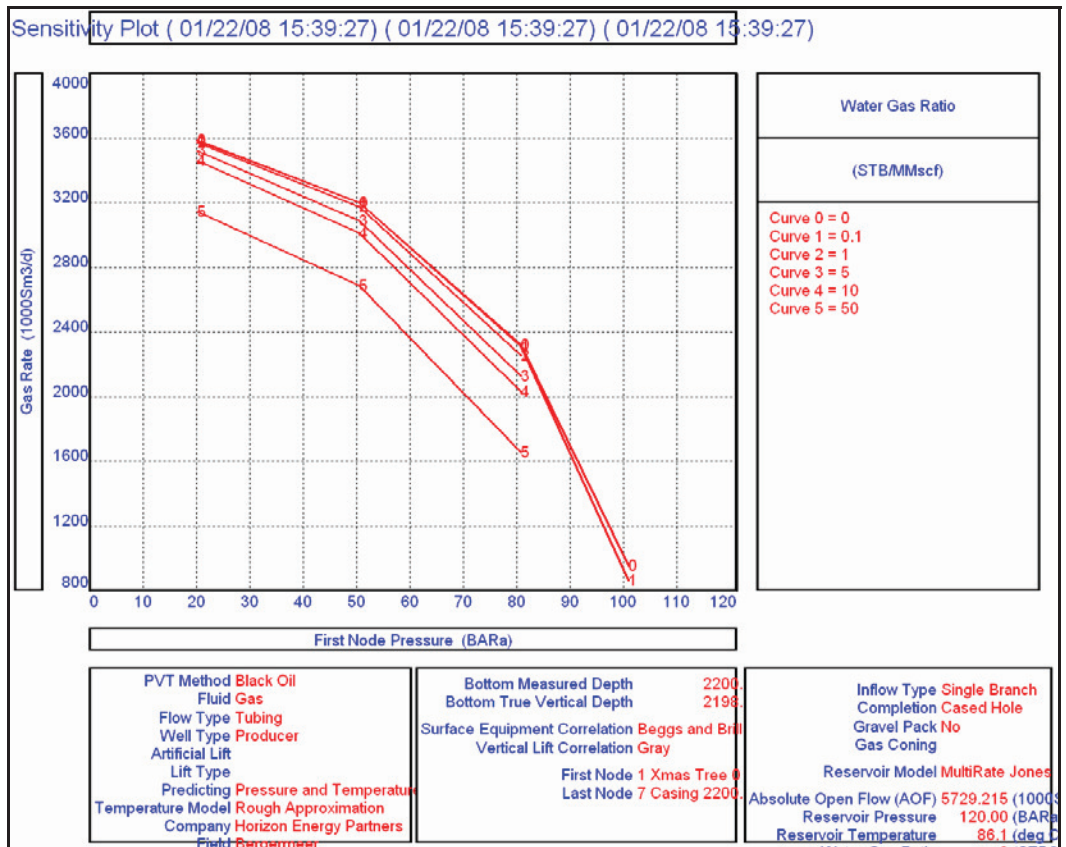


Figure 3-14 WGR sensitivity for vertical wells. The reservoir pressure is 157.5 bar.

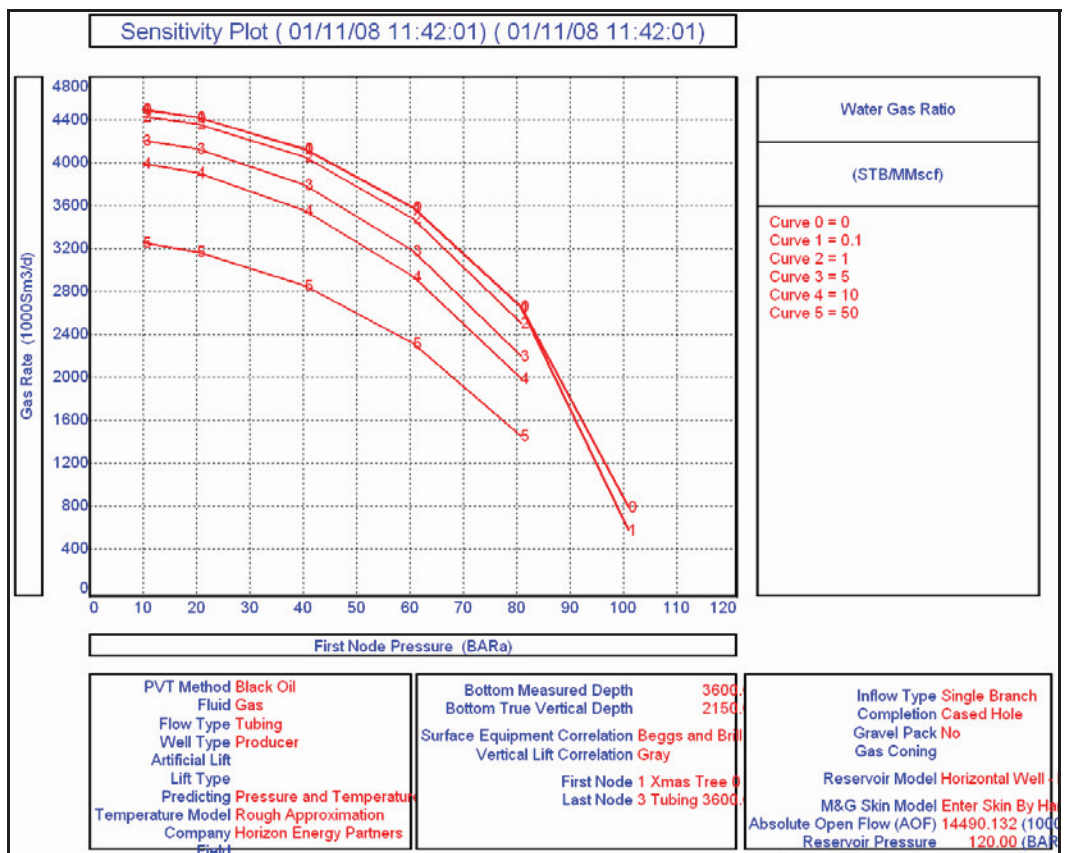


Figure 3-15 WGR sensitivity for horizontal wells. The reservoir pressure is 120 bar.

3.6.5 Tubing roughness

The tubing roughness can be seen to have a large impact. Originally, a roughness of 0.0005 inch was used for the lift-curves. The figure is based on the steel quality of the tubing in BGM-1. As the UGS will operate at higher rates it is important to limit the friction losses in the tubing. For our forecasts it is therefore assumed that stainless steel tubings will be used that have a roughness of ca 0.00015 inch. Figure 3-17 shows that at a moderate drawdown, the difference is 5% for the vertical well lift curves and ca 10% for the horizontal tubing. The vertical model has as main parameters Pres 120 bar, THP 80 bar, permeability 200 mD, CGR 0.5 stb/MMscf. The horizontal model has Pres 120 bar, THP 80 bar, permeability 50 mD, CGR 0.5 stb/MMscf.

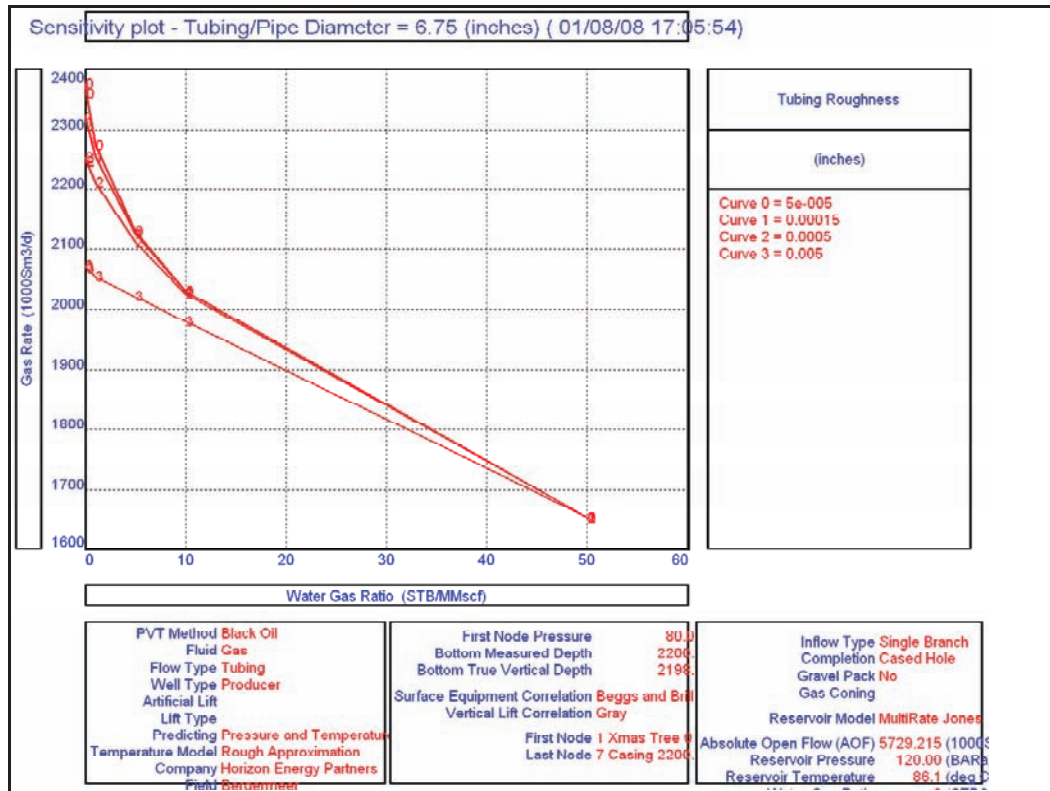


Figure 3-16 Lift curve sensitivity on roughness, Pres 120 bar, THP 80 bar, vertical well.

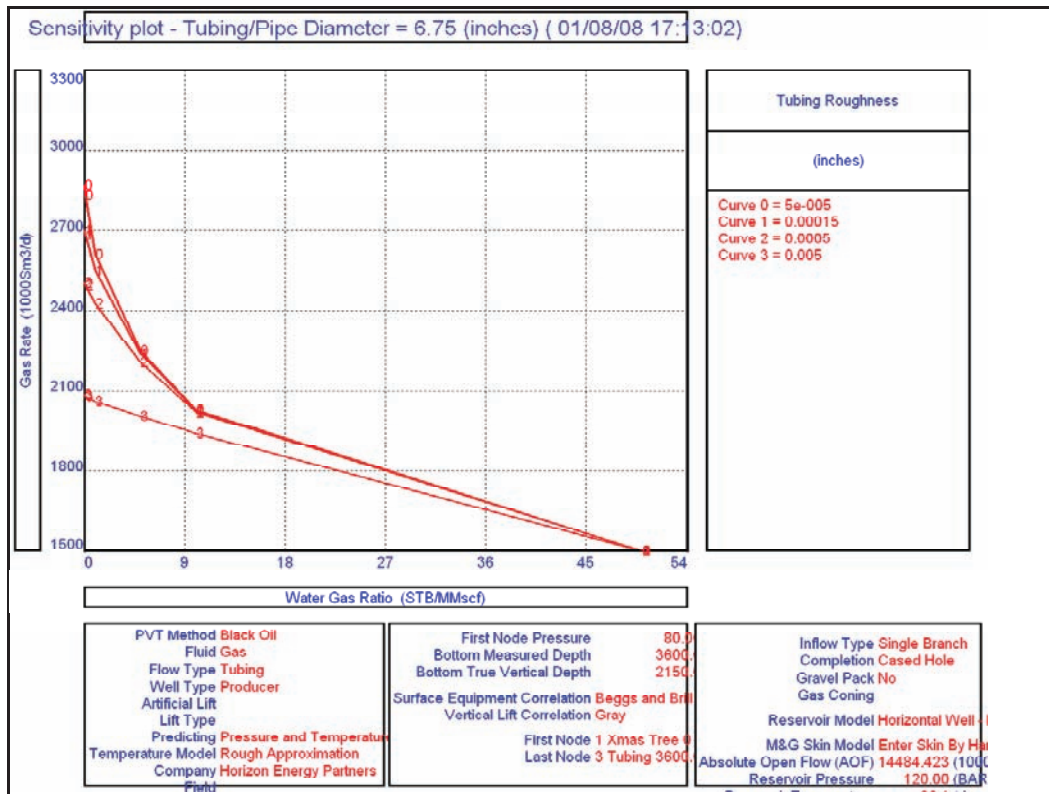


Figure 3-17 Lift curve sensitivity on roughness, Pres 120 bar, THP 80 bar, horizontal well.

3.6.6 Tubing diameter

The tubing used for both horizontal and vertical wells in the base case has a diameter of 7 5/8 inch. This was confirmed by the dynamic model of the UGS. As sensitivity, lift curves for larger tubings were run for the Medium, Large and XLarge cases in order to see how many wells would be needed. Results can be found in forecast sensitivities, section 5.4.1. In Figure 3-19, the vertical model has Pres 120 bar, THP 80 bar, permeability 200 mD, CGR 0.5 stb/MMscf. The horizontal model has Pres 120 bar, THP 80 bar, permeability 50 mD, CGR 0.5 stb/MMscf.

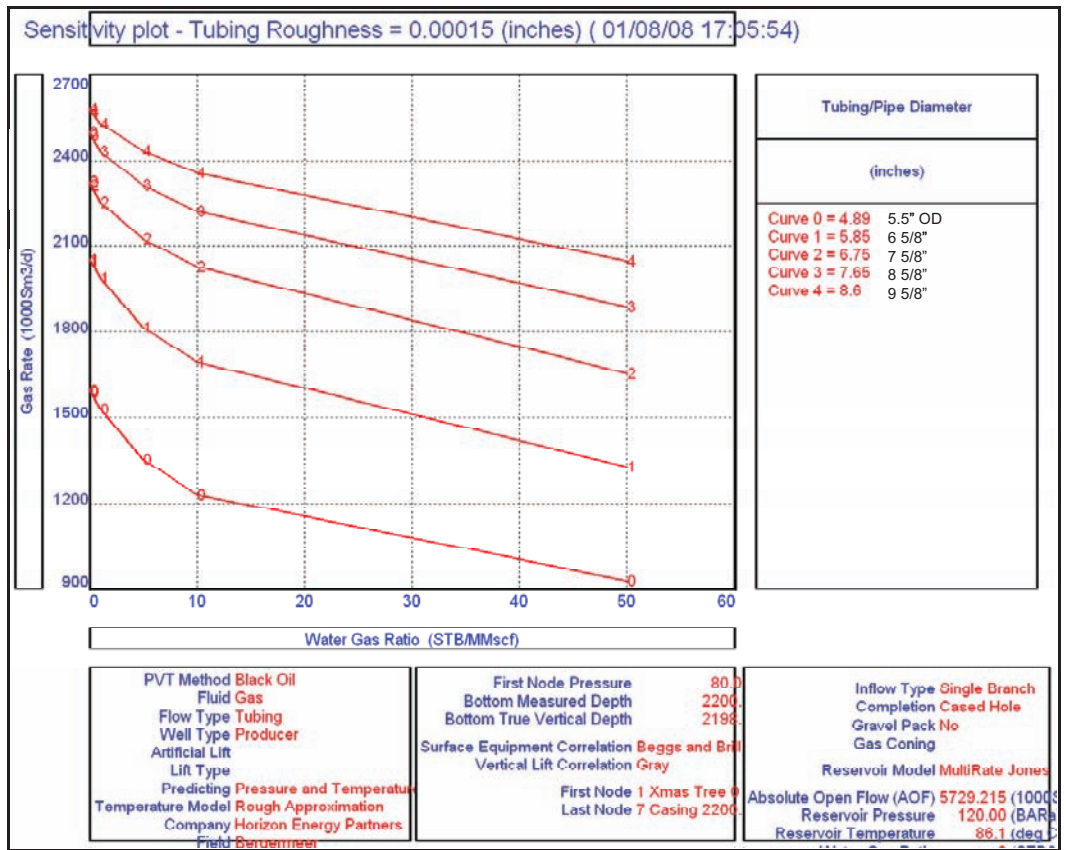


Figure 3-18 Lift curve sensitivity on tubing size, Pres 120 bar, THP 80 bar, horizontal well.

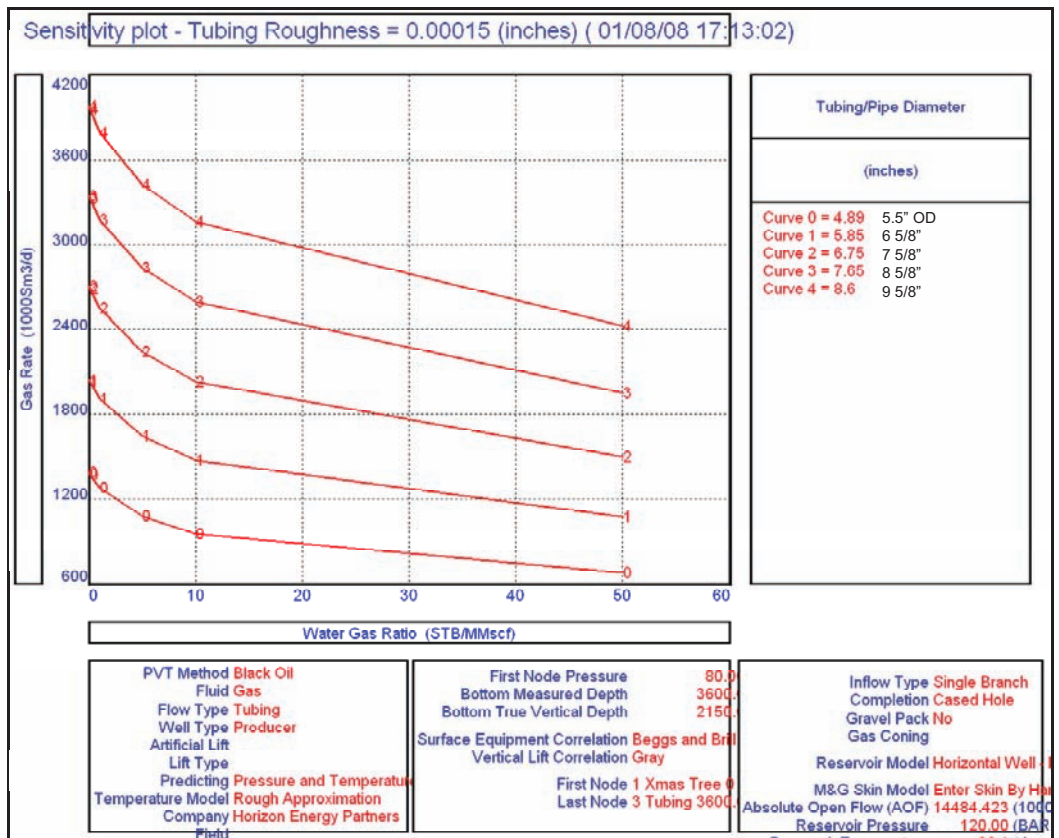


Figure 3-19 Lift curve sensitivity on tubing size, Pres 120 bar, THP 80 bar, vertical well.